Reman A, 2016, Quaternary stratigraphic framework of the Highland Valley Copper mine area, south-central British Columbia, BSc Thesis, U Waterloo, ON, 46 p.

NSERC-CMIC Mineral Exploration Footprints Project Contribution 101.

UNIVERSITY OF WATERLOO

Faculty of Science

QUATERNARY STRATIGRAPHIC FRAMEWORK OF THE HIGHLAND VALLEY COPPER MINE AREA, SOUTH-CENTRAL BRITISH COLUMBIA

Undergraduate Thesis

Prepared By:

Andrea Reman

ID: 20427980

April 6, 2016

Faculty Advisor:

Martin Ross

Associate Professor, Applied Quaternary Science

Abstract

At the Highland Valley Porphyry Cu-Mo mine in BC, a number of mineralized zones remain covered by thick unconsolidated sediments, mostly of Quaternary age, with the base extending into pre-Quaternary times. There is interest in characterizing these sediments to 1) determine whether a footprint of the buried mineralized zones can be detected in that cover, and also to 2) estimate the effect these sediments have on geophysical data reflecting the physical properties of the underlying bedrock. The goals of this study are currently focused on describing sedimentary successions from three drillcores in the vicinity of Highland Valley and determining the physical properties and establishing the provenance of thick diamicton units in these successions.

The methodology focuses on detailed sedimentological descriptions of three drillcores from the study area. Stratigraphic logs are integrated with available data and maps from government geological surveys. Laboratory analyses focus on textural (e.g. grain size), compositional (e.g. lithology) and geophysical characteristics.

A preliminary stratigraphic log has been created for the unconsolidated sediments at Highland Valley. The Cenozoic sediment successions have been interpreted to be deposited in glacial environments, as well as non-glacial and glacial lacustrine and fluvial environments. Diamicton units at one location were found to be stiff and dense (2.0 ± 0.2 g/cm^3) and very poorly sorted. The main bedrock source is igneous, and shows evidence of typical porphyry alteration, suggesting a local source. However, the magnetic susceptibility data differ considerably from that of local bedrock. The cause of this discrepancy is unclear and further research is needed to determine the exact bedrock source for the diamictons.

Acknowledgements

I would first like to thank my supervisor, Prof. Martin Ross for giving me the opportunity to work on this project and for all his much appreciated help and guidance throughout. Aaron Bustard at the BC Geological Survey gave a great deal of support as I attempted to make the most of my short time in the field. I am extremely grateful for their patience while they taught me a great deal. The magnetic susceptibility measurements done by Randy Enkin at the Geological Survey of Canada are greatly appreciated. Alain Plouffe at the Geological Survey of Canada, Travis Ferbey at the BC Geological Survey and Peter Winterburn at the University of British Columbia shared their findings from doing similar work in the area and gave helpful input. Special acknowledgement to Robert Lee from the University of British Columbia for setting up my field work and providing me with resources. Thanks go out to the employees of Highland Valley Copper Mine's core shack who welcomed me to work with their cores. I am also very appreciative of the research group of students of Martin Ross' who gave helpful suggestions and encouragement the whole way through. Funding through CMIC and the NSERC CRD program is gratefully acknowledged. ***CMIC-NSERC Exploration Footprints Contribution #101***.

Contents

Figures

Tables

1.0 Introduction

Highland Valley is a large porphyry Cu-Mo system located in the intermontane belt of British Columbia (**Figure 1**) (McMillan et. al., 2009). Large-scale mining began at the Highland Valley Copper Mine in 1962 (Bergey, 2009). Today it is owned and operated by Teck Resources Limited ("Teck", effective 97.5% interest) and the Highmont Mining Company (2.5% interest). The mine consists of several open pits (**Figure 2**).

Figure 1 The Highland Valley Copper Mine is located in south-central British Columbia (map imagery courtesy of Google Earth).

Figure 2 View of the Valley pit at the Highland Valley Copper Mine, viewed towards the southeast. The thick layer of unconsolidated sediments is shown.

The Highland Valley Mine is one of three mines at which the NSERC-CMIC-Footprints research project is conducted, due to it being one of Canada's most important ore deposit types (Integrated Multi-Parameter..., 2016). It is the largest mineral exploration research project ever undertaken in Canada, and aims to expand our knowledge of the footprint of deposits as well as develop methods to help the mining industry find hidden deposits, in order to increase Canada's accessible resources (Integrated Multi-Parameter..., 2016). Integrated multi-parameter proximal and distal footprints are characterized (Integrated Multi-Parameter..., 2016). Among these parameters are the characteristics of unconsolidated sediments overlying the footprint area. It is important to understand how these sediments affect and mask mineral deposits, to aid in facilitating more efficient and effective mineral deposit exploration for concealed mineral deposits.

2.0 Research Problem and Objectives

Some mineralized zones at Highland Valley occur beneath and around a partly buried paleo-valley, which contains more than 200m of unconsolidated, mostly Quaternary sediments. There is interest in characterizing physical and compositional properties of these sediments because thick deposits of unconsolidated cover make exploration for new mineralized systems particularly challenging. Not all is known about the valley fill successions, sediment transport, and depositional environments overlying buried mineralization and the associated alteration footprints. The processes involved in filling the valley may have eroded local bedrock (including alteration and mineralization), transported and deposited this material in different ways and at various distances from their source. Not much is known about whether the footprint of the buried mineralized zones can be detected in the overlying cover and what geochemical trace of the mineralization can be found in the surficial sediments. A thick and complex unconsolidated sediment cover such as the one at Highland Valley also affects geophysical mapping of buried mineralized zones and their alteration footprint. Geophysical data, such as magnetic and gravity, is collected to characterize the physical properties of underlying bedrock, but results are variably affected by the overlying cover. The unconsolidated cover has its own physical properties, and these may partly mask those of the targeted underlying bedrock.

Previous studies have looked at the glacial flow history in the area and the processes that resulted in the different sediment units were reconstructed (Plouffe et. al., 2012; Bobrowsky et. al., 1993; Fulton, 1975; Fulton, 1969; Fulton, 1967). It has also been concluded that the sediments burying the valley consist mostly of glaciolacustrine sediments (Bobrowsky et. al., 1993). Till geochemistry and indicator minerals have recently been used

to show that glacial sediments in the area do have traces of the porphyry mineralization that they overly, and these elements and minerals can be traced back to their mineralized zone source (Plouffe and Ferbey, 2015 [B]; Bouzari et. al., 2011). Despite substantial surficial geological work already having been completed at Highland Valley, there is still a knowledge gap regarding the subsurface stratigraphy, the physical properties of the different units, the provenance of subsurface tills, and how that ties in with the geological history put forth from surficial data by other workers. The ultimate goal in studying the unconsolidated sediments at Highland Valley is to improve exploration methods and approaches applied to exploration through transported cover.

The goals of this thesis are 1) describe the unconsolidated sediment successions around the Valley pit at Highland Valley Copper Mine, to determine their physical, sedimentological, geophysical and geochemical properties and 2) determine the depositional environments and the possible transport and sedimentation processes of targeted units partly filling the valley. The end result of a new set of petrophysical properties will hopefully be useful in constraining geophysical inversion. In addition, new insights into the sedimentology and composition of the main units and the mineralogy of the pebble fraction will be put forth to help advance understanding of provenance (bedrock sources) and identify the main transport/deposition processes and possibly, evidence of secondary (mechanical) dispersion of buried mineralization and its associated alteration footprint.

3.0 Background Geology

Highland Valley encompasses five of the mineralized zones of the region, and they are found at the core of the Guichon Creek batholith ("GCB") (Casselman et. al., 1995). This batholith is Upper Triassic and about 211 to 206 Ma in age, and the deposits are associated with the youngest two intrusive phases of it (d'Angelo, 2016). Mineralization of the deposits is estimated to have occurred between 206.7 ±1.5 Ma (Ash et. al., 2007). The GCB intrudes the Nicola Group (**Figure 3**), a unit of volcanic strata formed during the same period (Preto, 1979).

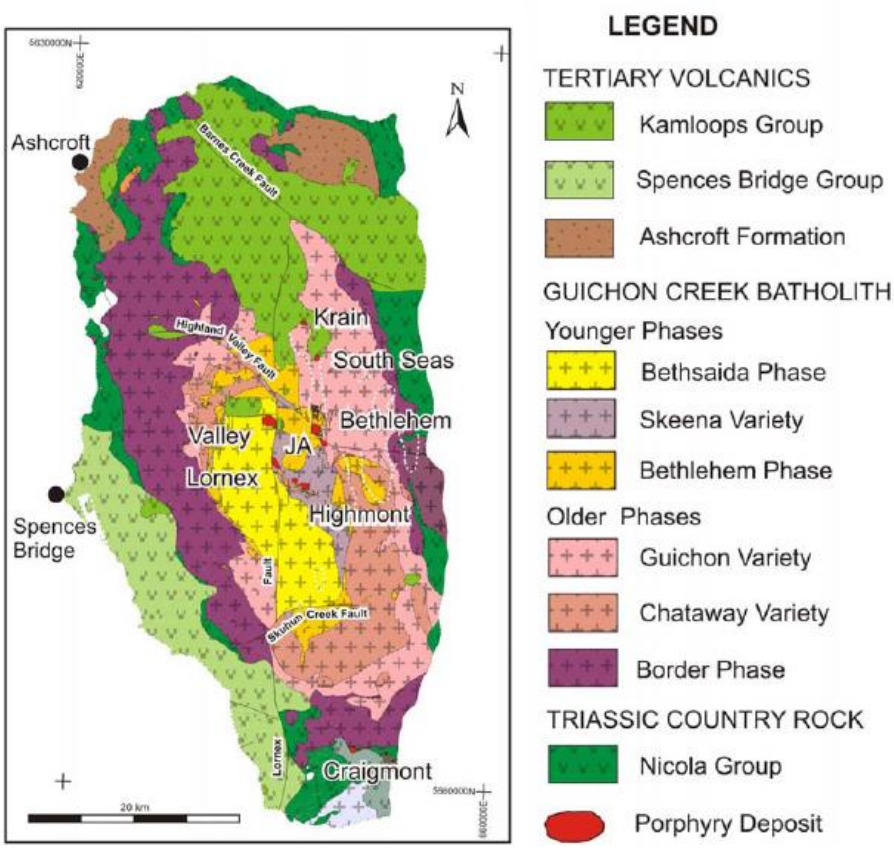

Figure 3 A bedrock map showing the deposits of Highland Valley that are found in the Guichon Creek Batholith, which is in turn hosted by the Nicola Group (McMillan et. al., 2009; McMillan, 1995).

Bedrock is overlain by Cenozoic sediments consisting of pre-Quaternary sediments at the base overlain by a thick succession of Quaternary sediments (Bobrowsky et. al., 1993) (**Figure 4**). The grey areas in the surficial geology map of figure 4 represent sediment with anthropogenic influence (e.g. waste rock, tailings). Among the grey areas on this map are the open pits and other mine activity areas (**Figure 5**). The glaciolacustrine (purple) and glaciofluvial (red) units are thick layers of unconsolidated sediments indicating the location of the main buried valleys in the study area. Outside of these valleys, till (green), or till veneer (light green), occurs at surface, as well as discontinuous bedrock outcrops.

The main ice flow direction in this region ranges from south to southeast (Plouffe and Ferbey, 2015 [B]). An ice divide formed north of Highland Valley, as a result of glaciers from the Coast and Caribou Mountains meeting (Plouffe and Ferbey, 2015 [B]). This divide was the source of ice flowing over Highland Valley (Plouffe and Ferbey, 2015 [B]).

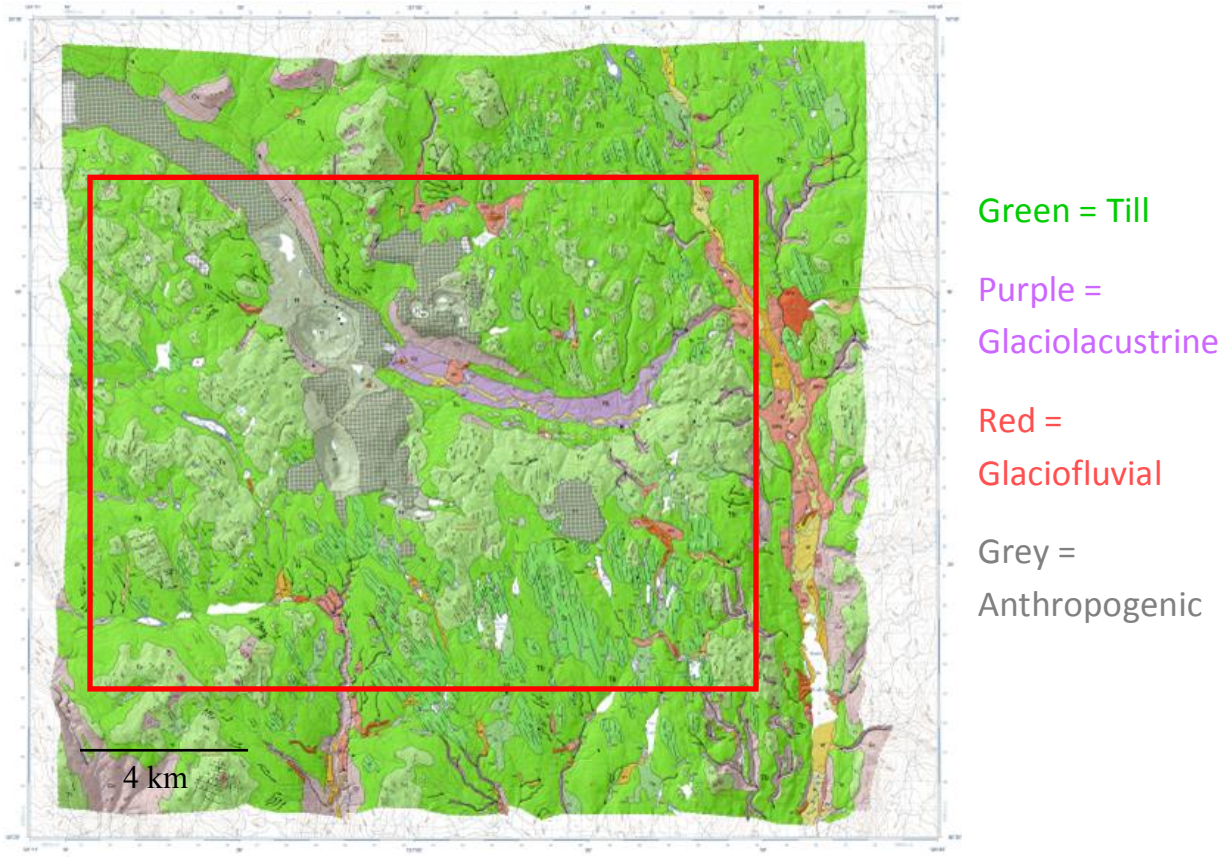

Figure 4 A surficial geology map showing the unconsolidated cover at Highland Valley (Plouffe and Ferbey, 2015 [A]). The red box shows the area encompassed by figure 5.

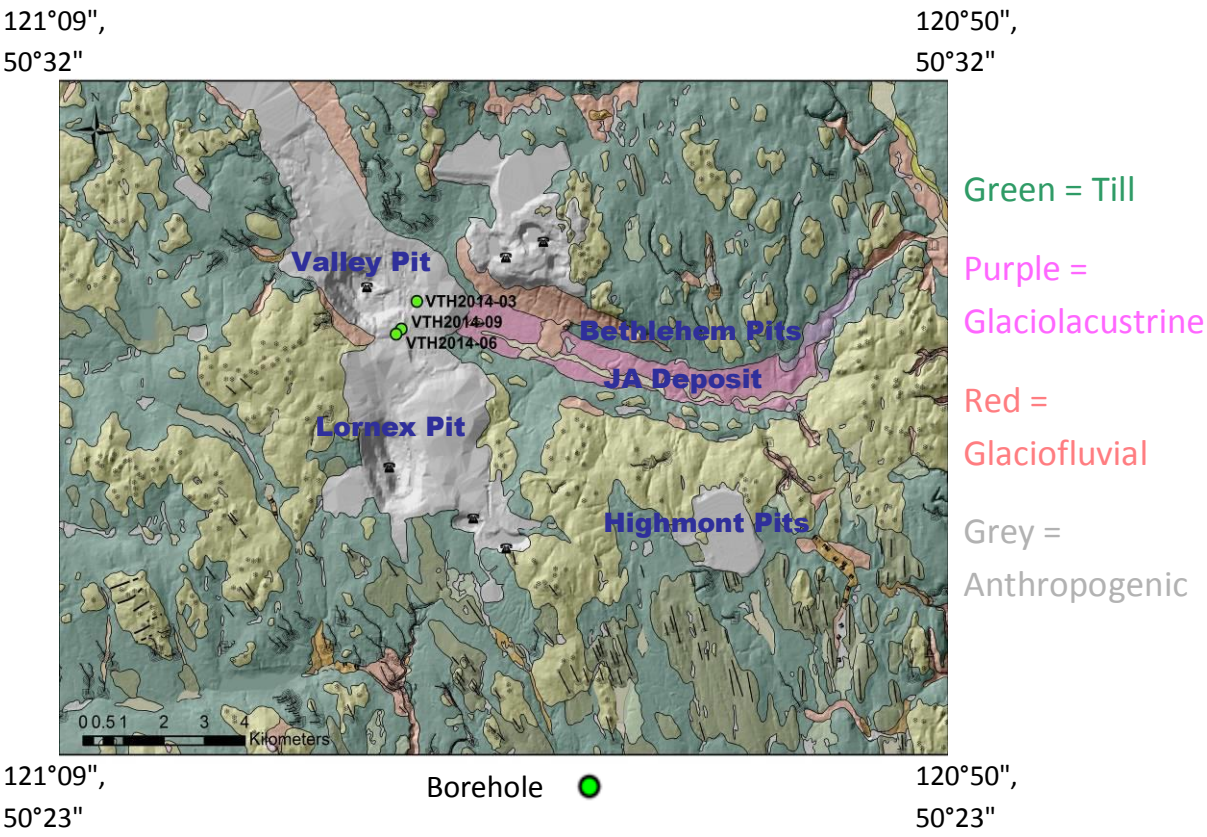

Figure 5 A close-up of the surficial geology map of figure 4 (see red box) showing the locations of the three boreholes from which cores have been logged as well as the locations of the open pits of the mine. Adapted from Plouffe and Ferbey (2015 [A]).

4.0 Research Methods

4.1 Investigation of Stratigraphy

Three rotosonically drilled cores from the study area were provided by Teck and logged at their core shack at the Highland Valley Copper Mine. Rotosonic drilling generally provides excellent recovery of Quaternary sediments, and sedimentary structures are also often preserved. The core is about 8.5cm in diameter. The core

lengths ranged from 124-235m, and 553m of total core (from 3 boreholes) was logged. The recovery was satisfactory, being about 80%.

A lithofacies analysis approach was used for logging the cores in the field. This technique consists of identifying marker beds, discontinuities and other unit contacts, and description of the overall texture of units and of their sedimentary structures using standard lithofacies coding schemes (Evans and Benn, 2004) (**Figure 6**). Three stratigraphic logs of the unconsolidated sediments in the study area were created using lithofacies analysis. Logging these cores from a stratigraphic point of view enhances the company's pre-existing geotechnical logs. High resolution photographs of the cores were also taken using a Nikon D5100 with a maximum resolution of 4,928 × 3,264 (16.2 effective megapixels).

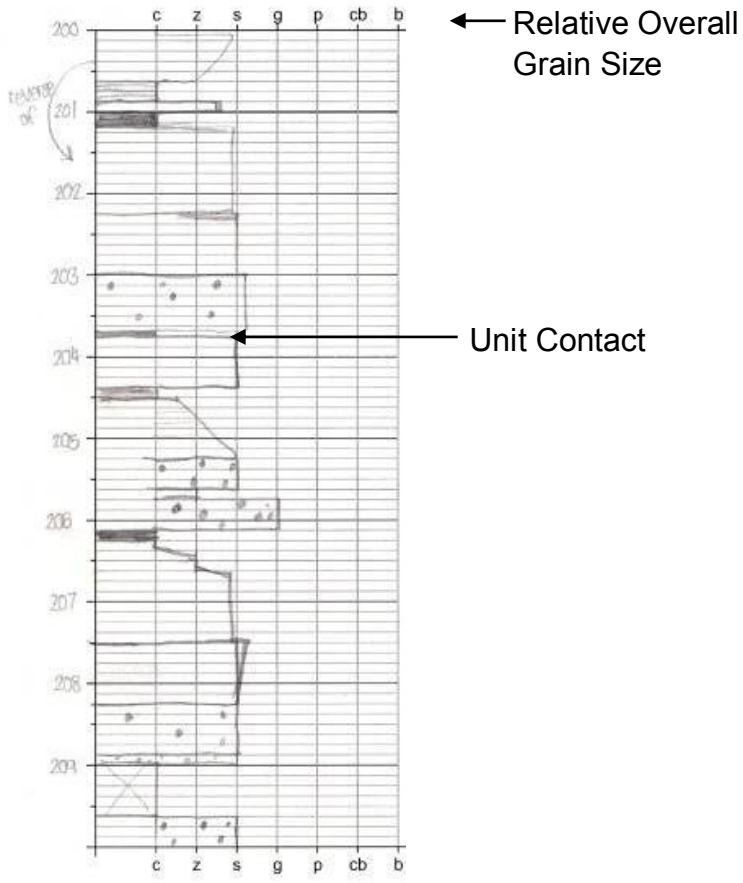

Figure 6 An example of the logging method of lithofacies analysis done on each core.

4.2 Investigation of Sedimentology

A detailed sedimentological analysis was carried out on the uppermost diamicton units of one of the cores (VTH2014-09) (cf. **Figure 5** for location). This was done by sampling these units and characterizing their different physical properties in the lab at the University of Waterloo.

First, the density of each sample was determined. Density was calculated in two ways; 1) using the dimensions of the sample along with its weight, and 2) using the

water volume displacement of the sample and its dry weight. In the second approach, the cores were wrapped with thin cling plastic wrap to prevent disaggregation of sediment. The diamicton cores are stiff and the material is of very low permeability. Therefore, water infiltration is minimal during the test, which lasted only few seconds.

Each sample was disaggregated and sieved into nine size fractions. Wet sieving had to be done first before dry sieving because the samples were stiff and difficult to break apart when dry (**Figure 7**). The water also helped flush out the small grains from amongst the larger ones, especially the silt and clay particles that tend to form coatings around larger clasts. The dry weight of each size fraction was measured. Laser diffraction was done on the fraction smaller than 63 μm to determine the proportion of that fraction of the sample belonging to subdivisions of that fraction. The laser diffractometer is a Fristch Analysette 22 with a full range from 2000 mm to 0.008 mm. Despite this wide range, these systems perform better in the fine range and are ideal for silt and clay, which are too small for sieving techniques. Grain size data were used to build full grain size curves and to analyse grain size distribution and statistics. The phi scale is a logarithmic scale defined by $\Phi = -\log_2(d)$ where Φ is the phi scale and d is the diameter of the particle in mm (Boggs, 2006). The mean grain size and standard deviation were calculated, both using the method of moments. The method of moments is a mathematical method comprised of formulas for calculating grain size parameters directly from the grain size data (Boggs, 2006).

Figure 7 Wet sieving was done on the disaggregated samples.

Finally pebbles (4-8mm and >8mm) were examined to determine their lithology. They were subdivided and counted based on the following lithology types: coarse-grained igneous, fine-grained igneous, aphanitic igneous, porphyritic, sedimentary and aphanitic igneous/sedimentary.

4.3 Investigation of Magnetic Susceptibility

Magnetic susceptibility measurements of the core samples were done by Randy Enkin at the Geological Survey of Canada. These were done using a SM20

Susceptibility Meter on the full width of the core and the Bartington MS2E Probe on the pebbles in the core.

5.0 Results

5.1 Stratigraphy

5.1.1 Core VTH2014-03

Core VTH2014-03 (**Figure 8**) is 124.2m long and consists of well-sorted units, with the exception of a small number of thin diamicton units near the top. The bottom unit consists of subrounded to rounded cobbles and gravel, and its thickness is about 8m. A thin layer of gravelly coarse sand with rounded to subangular clasts overlies this. This is overlain by a poorly consolidated thick laminated clayey silt unit measuring about 14m. Each laminae is about 2-3mm thick. The majority of the core consists of sand units. The next to be deposited was a fine sand unit about 3m thick. It contained fine laminations and cm-scale bedding, as well as rounded pebbles about 5cm in diameter in the bottom 5cm of this unit. This is overlain by another very thick unit of gravelly coarse sand with very poor consolidation. It measures about 61m in thickness. The coarse gravel particles are about 5cm in diameter. It is interrupted by a 10m thick layer of rounded to subangular pebbles up to 5cm in diameter. A relatively thin (about 1.5m) layer of finely laminated silty clay is found on top of this. Layers of sand of varying coarseness and thickness and sometimes with pebbles or granules fill the next 21m upwards in the core. This is overlain by a thin, 1.5m thick, diamicton unit with a fine sand matrix and granules to boulders measuring about 10cm. Thin diamicton units are found at the top of the core, interlayered with thin layers of

pebbles and cobbles. The pebbles and cobbles are subrounded to subangular, and most consist of phaneritic or aphanitic rocks. See figures 2-4 in the appendix for photos of the units.

The bottom gravel and cobble layer at the base of the succession, middle pebble layer and pebble and cobble layers near the top of it are interpreted to be deposited in a high-energy fluvial system. Due to the large size of the clasts making up this unit, a high amount of energy is needed to transport them. The different sand layers throughout the core are also interpreted to be fluvial (or glaciofluvial) in origin, although some of the thick layers could record deltaic deposition. The presence of horizontal bedding in places suggests some sand layers may represent upper plane beds and the occurrence of pebbles throughout the sand units also provide further evidence of upper flow regime (100-150 cm/sec). The thick laminated clayey silt unit and the thin layer of finely laminated silty clay overlying the coarse bed near the base of the core most likely record a lacustrine environment. This is based on the rhythmicity of the laminae and their general texture, which are typical of lacustrine successions. The laminae show no sign of bioturbation, and as such it is interpreted that the environment of deposition was likely in a cold lake environment. The interstratifications of silt and clay and minor fine sand ripples (Fig. 8) could represent low-density turbidity currents, alternating traction and settling processes with seasonal variations of inflow energy and sediment yield.

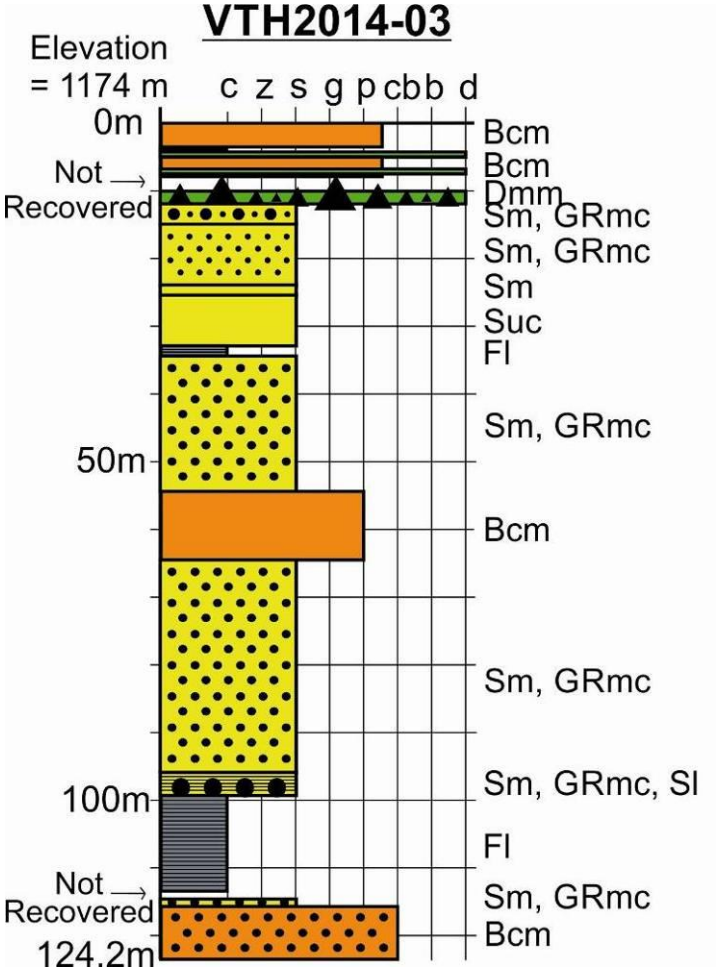

Lithofacies Codes

Dmm=Matrix-supported, massive diamicton

Bcm=Clast-supported, massive boulders

Dms=Matrix-supported, stratified diamicton

Gm=Clast-supported, massive gravel

GRmc=Massive granules with isolated, outsize clasts

St=Medium to very course and trough cross-bedded sand

Sl=Sand with horizontal and draped lamination

Sm=Massive sand

Suc=Upward coarsening sand

Fl=Finely laminated silts and clays, often with minor fine sand and very small ripples

Flv=Finely laminated silts and clays with rhythmites or varves

Fm=Massive silts and clays

Figure 8 Stratigraphic log of core VTH2014-03. See Figure 5 for location. Lithofacies codes from Evans and Benn (2004).

5.1.2 Core VTH2014-06

Core VTH2014-06 (**Figure 9**) consists of mostly thin units of varying grain sizes. It is 194m long, however not all of it was available for logging. The base of the succession is composed of thin layers of sand up to 4m thick alternating with very fine layers of silt and clay less than 1m thick and coal horizons up to 40cm thick. The sand ranged from fine to coarse, and sometimes included coarsening or fining upwards sequences, laminae of organic materials up to about 3cm thick as well as pebbles up to about 3cm in diameter. The clay contained laminations or was organic rich in places. The silt was clayey and occasionally contained organic-rich horizons up to about 8cm thick as well as organic roots. The units recovered near the top of the core included a 12m thick layer of rounded, aphanitic and phaneritic boulders and cobbles up to 23cm in diameter. The remaining layers were thin and consisted of varying sediment sizes. Rhythmic beds of silt and clay up to 1cm thick were observed. There were fine to coarse sand layers that were either well or poorly sorted and occasionally contained fine laminations, very crude beds, coarsening upward sequences, cobbles or pebbles. Well-rounded aphanitic and phaneritic cobble, pebble, gravel and granule layers are present. See figures 5-7 in the appendix for photos of the units.

The layers composed of granule-to-boulder sized fragments indicate a fluvial system. The larger size and rounding of these particles suggest a high energy depositional environment. A slower fluvial system most likely transported the different sand layers throughout the core. The presence of bedding, coarsening or fining upward sequences and pebbles or boulders clearly indicates varying energy of flow. The thin silt and clay layers most likely record a lacustrine environment. A fluvial system along

with a deepening and shallowing lacustrine system would have possibly deposited this sequence. The lake resulted in the lamination of fine material, and had organic matter input. The base of the lacustrine unit is organic-rich and lacks bioturbation structures, which suggests a closed lake basin with stratified water masses with low-oxygen (anoxic) bottom waters that favored preservation of organic matter. Decreasing organic matter up the sequence suggests an increase in oxygen levels at the bottom of the lake, but the continued undisturbed laminations (no bioturbation) indicates a cold lake environment. The presence of sandy rhythmites with isolated rounded pebbles likely indicates a glacial lake (ice-contact setting) with dropstones from floating icebergs.

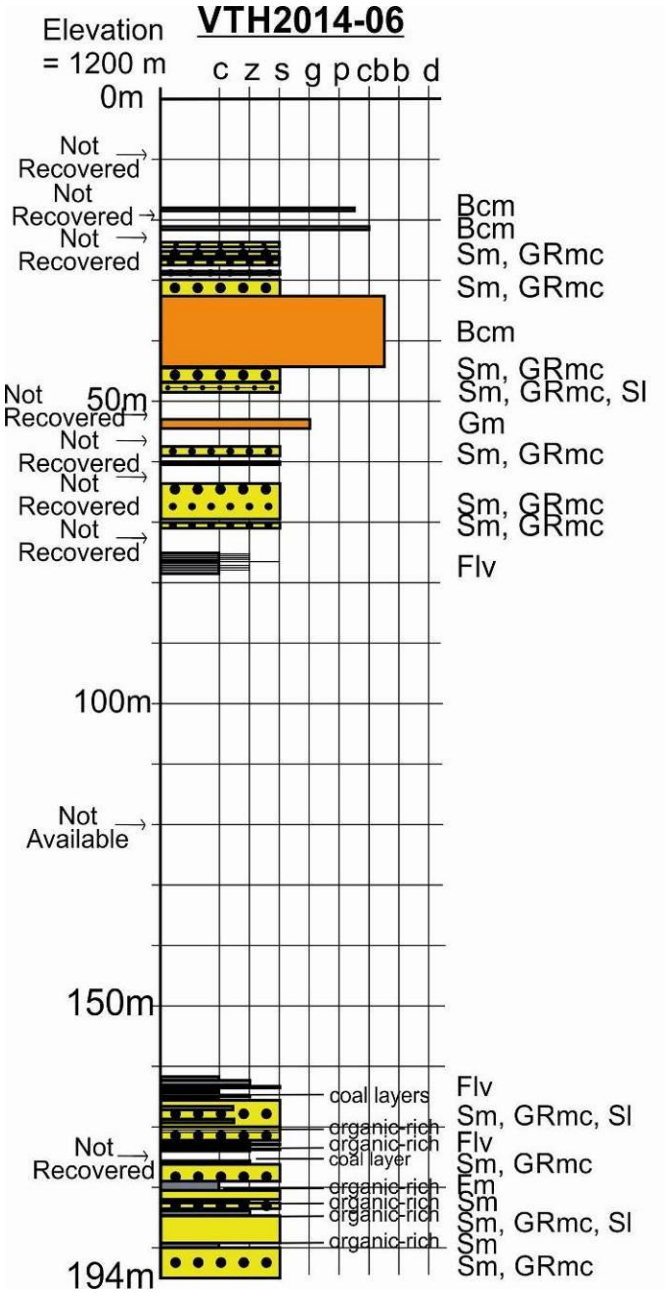

Lithofacies Codes

Dmm=Matrix-supported, massive diamicton

Bcm=Clast-supported, massive boulders

Dms=Matrix-supported, stratified diamicton

Gm=Clast-supported, massive gravel

GRmc=Massive granules with isolated, outsize clasts

St=Medium to very course and trough cross-bedded sand

Sl=Sand with horizontal and draped lamination

Sm=Massive sand

Suc=Upward coarsening sand

Fl=Finely laminated silts and clays, often with minor fine sand and very small ripples

Flv=Finely laminated silts and clays with rhythmites or varves

Fm=Massive silts and clays

Figure 9 Stratigraphic log of core VTH2014-06. See Figure 5 for location. Lithofacies codes from Evans and Benn (2004).

5.1.3 Core VTH2014-09

The base of core VTH2014-09 (**Figure 10**) is characterized mostly by thin intervals of sand and by interspersed laminated silts and clays. It is coal rich. The lowermost diamicton layer is about 46m thick and is pebble-rich with a silt and clay matrix. There is one thick sand (about 54m) bed near the middle of the core. Several diamicton layers are present near the top of the core, and are up to 11m thick. These diamictons have a clayey fine sand matrix, which is coarser than that of the deeper diamicton. All the diamicton units are matrix- supported and stiff. The texture shows evidence of little reworking at the depositional site. Mostly subrounded to subangular, as well as rounded clasts, were found in the top diamicton units. Angular clasts were found in the bottom diamicton unit, as well as large, shattered clasts. The top of core VTH2014-09 is composed of pebble to boulder sized fragments of rock. See figures 8-14 in the appendix for photos of the units.

The interstratified sand, silt and clay units at the bottom of the succession most likely indicate fluvial and lacustrine environments. Changing lake levels would determine which one was present at a certain time.

The top diamicton layers are confidently interpreted as subglacial traction till units on the basis of their overall sedimentological character including grain size distribution (cf. sect. 5.2.1), stiffness and density (cf. sect. 5.2.2), pebble shape and lithology (cf. sect. 5.2.3), which together suggest long transport but little to no water involved. The presence of preferentially oriented clasts records the strain history of the

diamicton with stress aligning particles in a preferred orientation. This is also a common feature of subglacial tills (Benn and Evans, 2010).

The bottom diamicton unit is interpreted to be a landslide breccia. The lack of variety in the lithology of the clasts as well as their angularity and the presence of large pieces of shattered rock suggest transport over a short distance with little water involved.

Graded bedding was seen in the sand units of this core. This occurs when the energy of transport varies. Due to the very large size and rounding of the topmost pebble to boulder sized fragments of rock, it seems likely that they are fluvial in origin. It is probable that this flowing water would have been glaciofluvial due to the close stratigraphic proximity of till units. Glacial rivers would have formed after the melt and retreat of the ice sheet that deposited the diamicton units underneath the sand and boulder layers, and deposited the sand and boulder units. A glacial lake formed from the meltwater could have been the environment forming all the silt and clay layers.

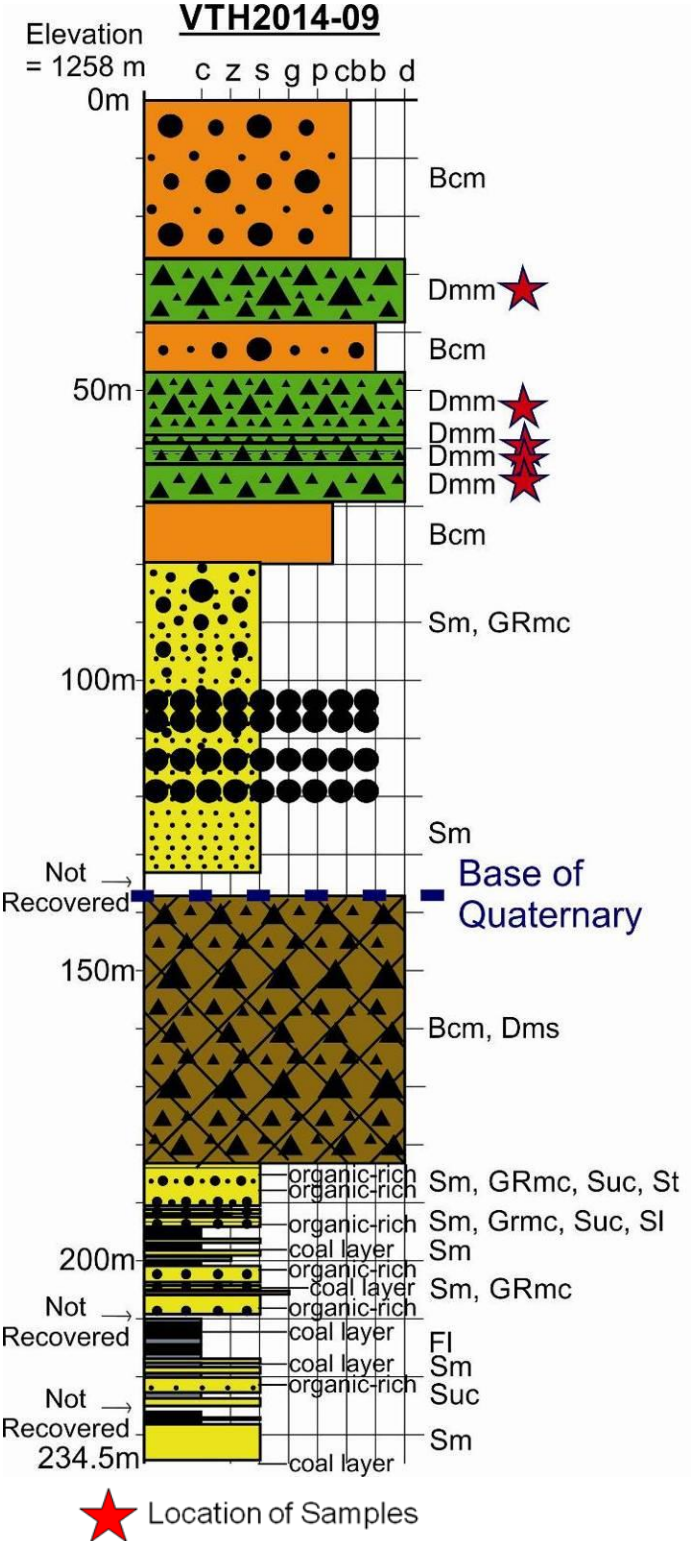

Lithofacies Codes

Dmm=Matrix-supported, massive diamicton

Bcm=Clast-supported, massive boulders

Dms=Matrix-supported, stratified diamicton

Gm=Clast-supported, massive gravel

GRmc=Massive granules with isolated, outsize clasts

St=Medium to very course and trough cross-bedded sand

Sl=Sand with horizontal and draped lamination

Sm=Massive sand

Suc=Upward coarsening sand

Fl=Finely laminated silts and clays, often with minor fine sand and very small ripples

Flv=Finely laminated silts and clays with rhythmites or varves

Fm=Massive silts and clays

Figure 10 Stratigraphic log of core VTH2014-09. See Figure 5 for location. Lithofacies codes from Evans and Benn (2004).

5.2 Sedimentology

5.2.1 Grain Size Analysis

Cumulative grain-size curves were produced by combining sieving and laser results for each diamicton sample (**Figure 11**). There is a varying amount of grains larger than -3Φ or 8mm for each sample. The curves become less steep at 4-6Φ, showing that there is relatively less material of this size, which corresponds to the coarse silt fraction. The silt in all these samples is mostly fine silt. The curves begin tapering off and reaching 100% at about 9Φ, which is medium-sized clay. There is some coarse-sized clay in these samples, but not much fine-sized clay.

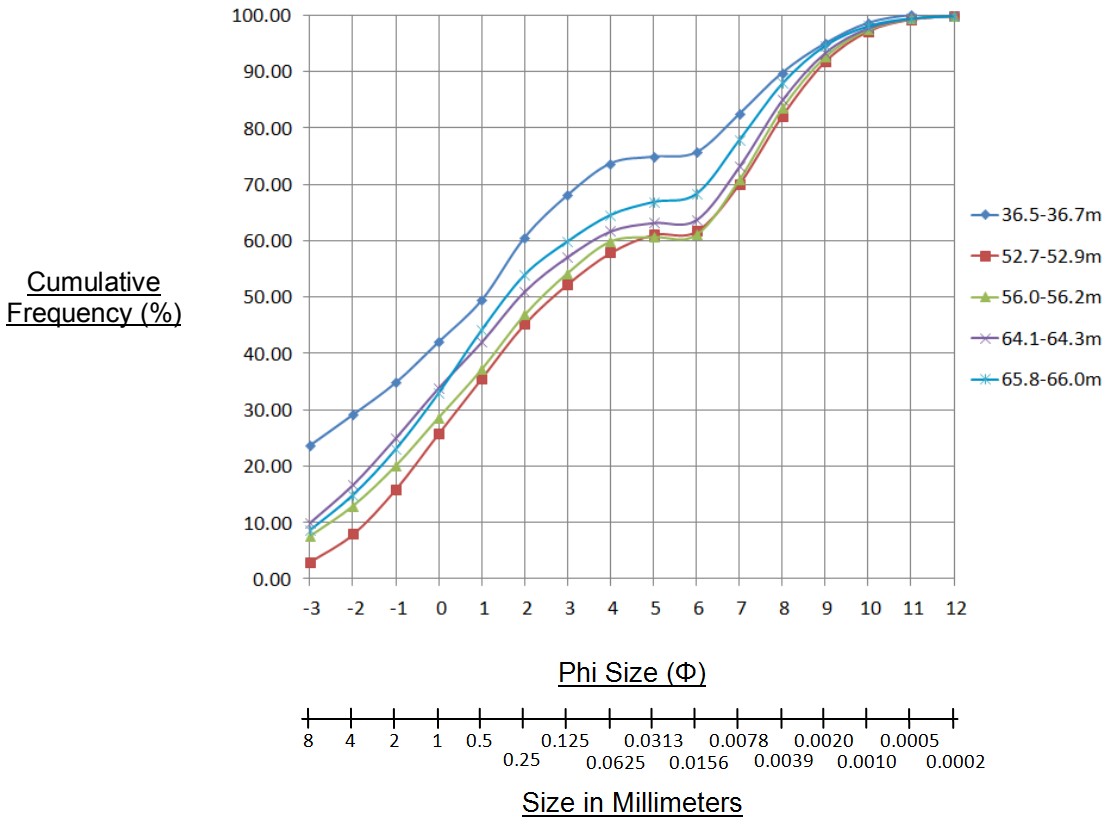

Figure 11 Cumulative grain size curves of the samples.

The mean grain size ranged from 0.24-0.62mm, which is part of the sand-sized range and around the middle of the entire range of grain sizes from boulders to fine clay (**Table 1**). The phi standard deviation values indicate that the samples are very poorly sorted (corresponds to a phi standard deviation between 2.00 and 4.00Φ).

Table 1 Mean grain size and standard deviation for each sample.

Sample Depth (m)	Mean Grain Size (mm)	Standard Deviation (Φ)
36.5-36.7	0.62	3.11
52.7-52.9	0.24	2.55
56.0-56.2	0.28	2.76
64.1-64.3	0.35	2.91
65.8-66.0	0.36	2.80

The <63µm fraction of each sample was analyzed with a laser diffractometer to complete the grain size curve, and provided a more detailed breakdown of the distribution of grain size of the silt and clay fractions (see appendix figures 15 and 16). The grain size distributions of the silt and clay fraction of the four samples are similar. These curves range from 0.063mm to 0.0008mm, and their frequency corrected for the total weight of the sample had a mode at or approaching 10µm or 0.01mm, with a tail decreasing towards 0.0001mm. There is another but much smaller mode at about 40µm or 0.04mm, which is the size of coarse silt.

5.2.2 Density

The density of each sample was measured using both the volume from its dimensions and from its displacement in water and sample dry weight (cf. Method section 4.2). The mid-value of these two density values was taken as the final density value for each sample (**Table 2**). The samples are all from the upper diamicton units of

core VTH2014-09. The density values are quite high for unlithified sediments. The diamictons are also stiffer than they should be for their depth. The density values are consistent with this apparent stiffness. In addition, a close look at the grain size curves shows that the proportion of large clasts (>4mm), which have a higher density than the matrix, is above 10% for four of the five samples, with one being as much as 30%. These samples did seem to be highly compacted given their stiffness, and they were also visually clast-rich (see section 6.1), including many large pebbles.

Table 2 Density of the samples, all of which were collected from the upper diamicton units of core VTH2014-09. Final density for each was calculated using the mid-value of the densities each using one of the two different methods. Density using volume from displacement is not very precise due to lack of detailed markings on the beaker used.

Sample Depth (m)	Density using Volume from Dimensions (g/cm^3)	Density using Volume from Displacement (g/cm^3)	Final Density (g/cm^3)
36.5-36.7	2.2	2.2	2.2
52.7-52.9	2.0	2.2	2.1
56.0-56.2	1.8	2.2	2.0
64.1-64.3	1.9	2.2	2.0
65.8-66.0	1.5	2.2	1.9

The mid-value of the densities calculated using the two different methods was used, due to the roughly equal amount of error on both. The density using volume from dimensions was not perfectly accurate because of the irregularity of the shapes of the cores. The density using volume from displacement had error because of the limited detail of the markings on the beaker. The density of these samples generally decreased with increasing depth for the method of calculation using dimensions (**Figure 12**).

The shallowest sample, from 36.5 to 36.7m, had the highest density. It also had the highest proportion of large clasts (**Figure 11**). This sample having the highest proportion of clasts larger than 8mm can explain why it also has the highest density, because rock has a higher density than the unconsolidated matrix.

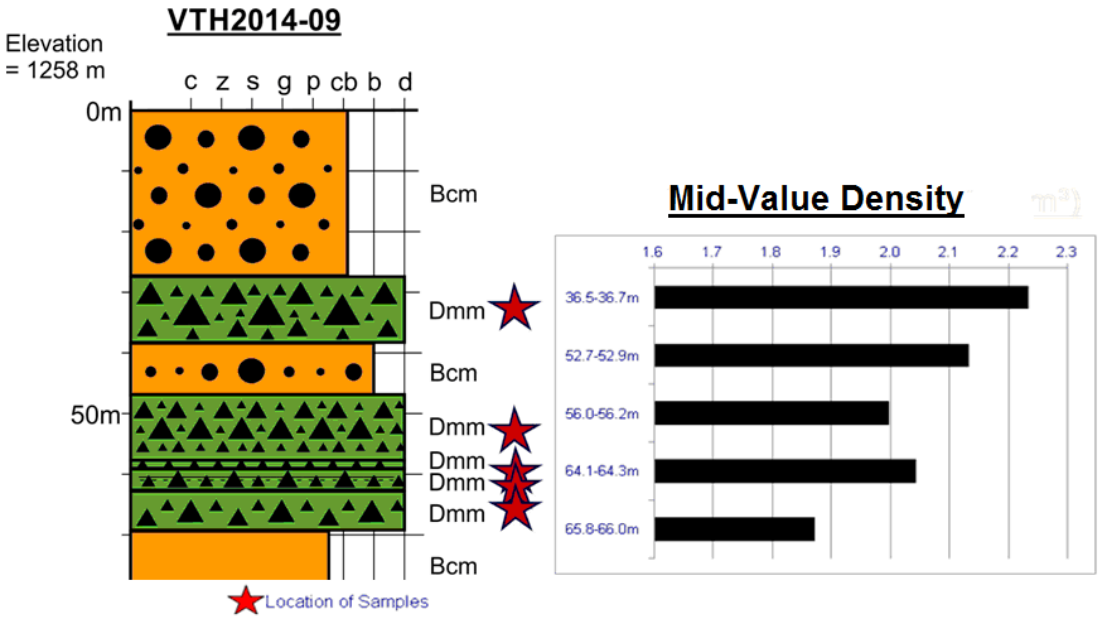

Figure 12 A graph showing density vs. depth of the samples.

5.2.3 Pebble Lithology

The vast majority of the pebbles >4mm in each sample was coarse-grained igneous (**Figure 13**). Fine-grained igneous made up a significant proportion of the pebbles for most of the samples. A few porphyritic pebbles were also found in each of the samples, which reflect specific magmatic processes and can narrow down the area from which these pebbles are sourced from.

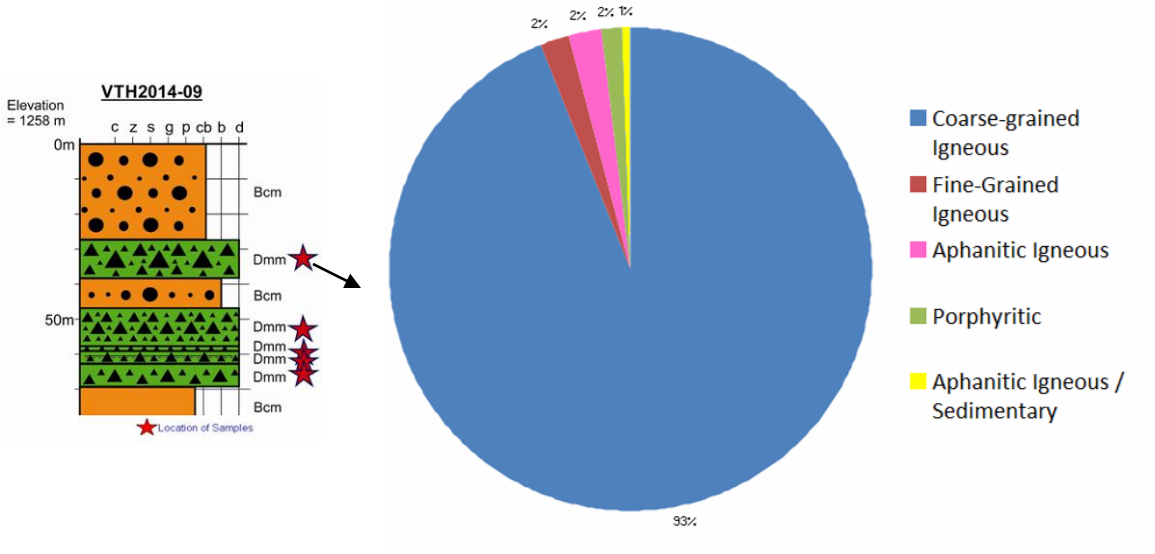
VTH2014-09
Elevation = 1258 m
c z s g p cb b d
0m
50m
Bcm
Dmm
Bcm
Dmm
Dmm
Dmm
Dmm
Bcm
Location of Samples
2%
2%
2%
1%
93%
Coarse-grained Igneous
Fine-Grained Igneous
Aphanitic Igneous
Porphyritic
Aphanitic Igneous / Sedimentary

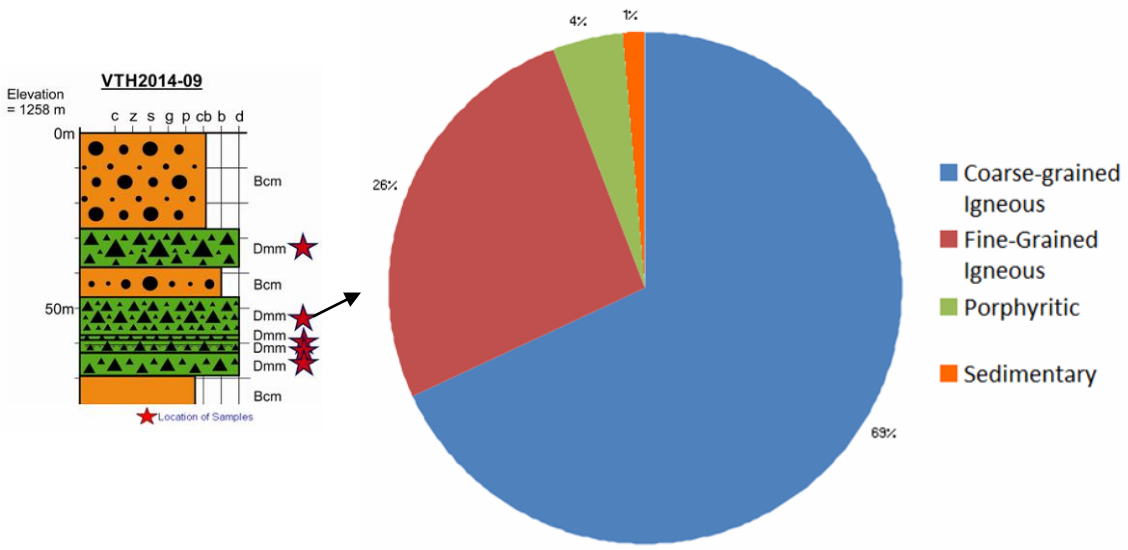
VTH2014-09
Elevation = 1258 m
c z s g p cb b d
0m
50m
Bcm
Dmm
Bcm
Dmm
Dmm
Dmm
Dmm
Bcm
Location of Samples
4%
1%
26%
69%
Coarse-grained Igneous
Fine-Grained Igneous
Porphyritic
Sedimentary

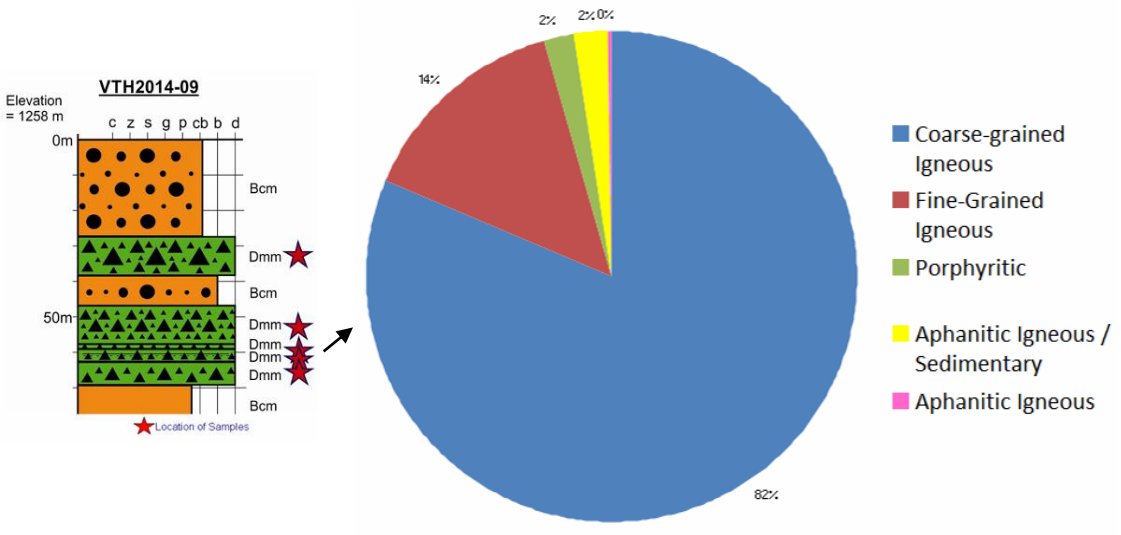
VTH2014-09
Elevation
= 1258 m
c z s g p cb b d
0m
50m
Bcm
Dmm
Bcm
Dmm
Dmm
Dmm
Dmm
Bcm
Location of Samples
2%
2%
14%
82%
Coarse-grained Igneous
Fine-Grained Igneous
Porphyritic
Aphanitic Igneous / Sedimentary
Aphanitic Igneous

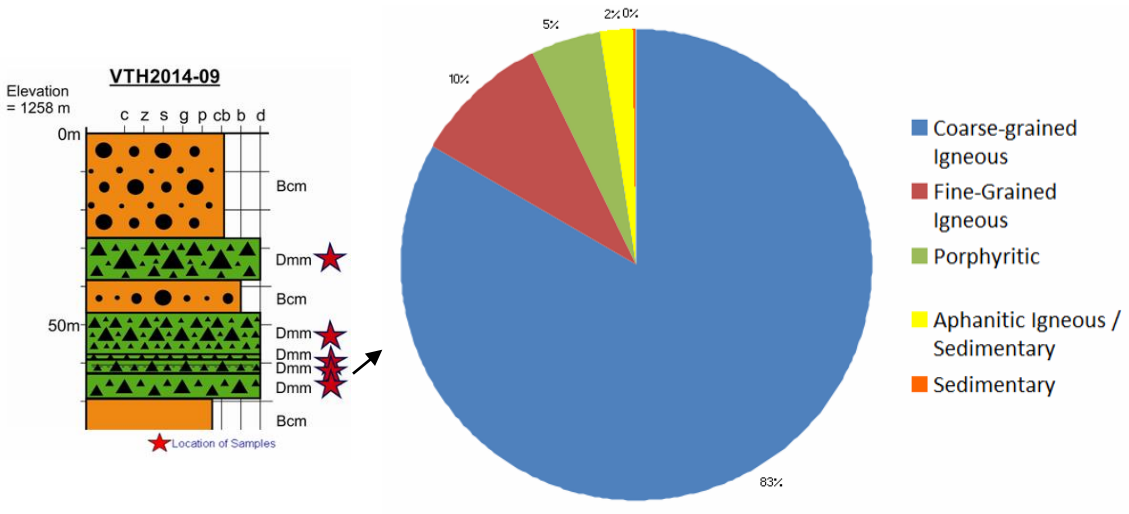
VTH2014-09
Elevation
= 1258 m
c z s g p cb b d
0m
50m
Bcm
Dmm
Bcm
Dmm
Dmm
Dmm
Dmm
Bcm
Location of Samples
5%
2%
10%
83%
Coarse-grained Igneous
Fine-Grained Igneous
Porphyritic
Aphanitic Igneous / Sedimentary
Sedimentary

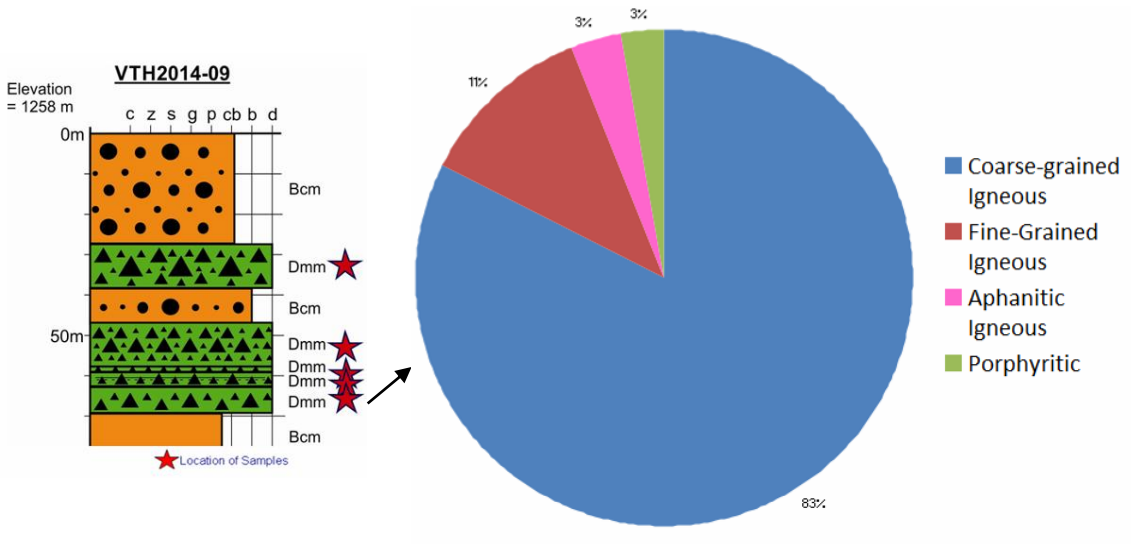

Figure 13 Composition and proportion of pebbles >4mm from each sample in core VTH2014-09.

The dominant pebble type in all of these samples is a coarse grained felsic igneous rock (**Figure 14**). It consists of large coarse grains of quartz, smaller coarse grains of feldspar, and minor amounts of fine-grained small black minerals and sometimes very fine sized muscovite. This rock shows orange-mottled coloured weathering on its surface.

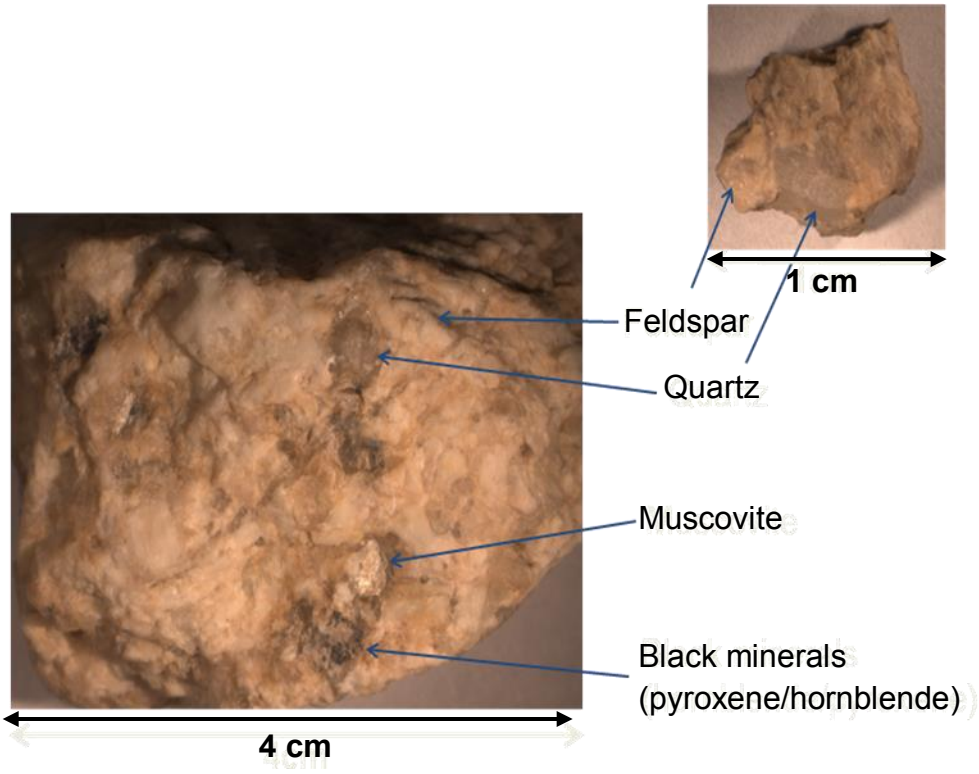

Figure 14 Photos of the dominant pebble type in the samples.

The top diamicton units of core VTH-2014-09 from which these samples are taken from are interpreted to be tills as opposed to slumps or rockfalls. The combination of striated clasts, iron and bullet shaped clasts with a truncated facet, as well as the subangular and polymict (multiple lithologies) nature of the clasts support this interpretation. These diamictons were thus produced through erosion, transport and sedimentation associated to glacial processes.

Chlorite, epidote, quartz, feldspars, hematite, magnetite and carbonates are all important alteration minerals for porphyry copper deposits (Sillitoe, 2010) (**Figure 15**). They were all found in small amounts in many of the rock types of each sample. Widespread propylitic alteration is common in porphyry deposits, and is characterized

by green colour due to the presence of green chlorite, pistachio-green epidote and greenish-black actinolite (Taylor, 2009) (**Figure 16**). The presence of these alteration minerals is most likely the result of alteration of the mineralized zones of the Highland Valley porphyry system.

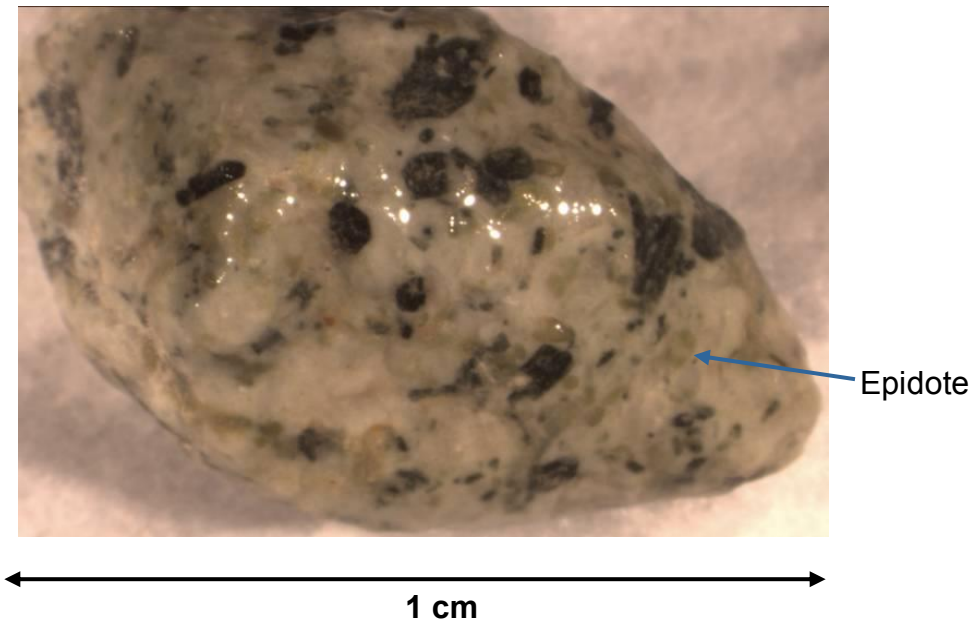

Figure 15 Photo of a pebble showing epidote grains from the sample at a depth of 65.8-66.0m in core VTH2014-09.

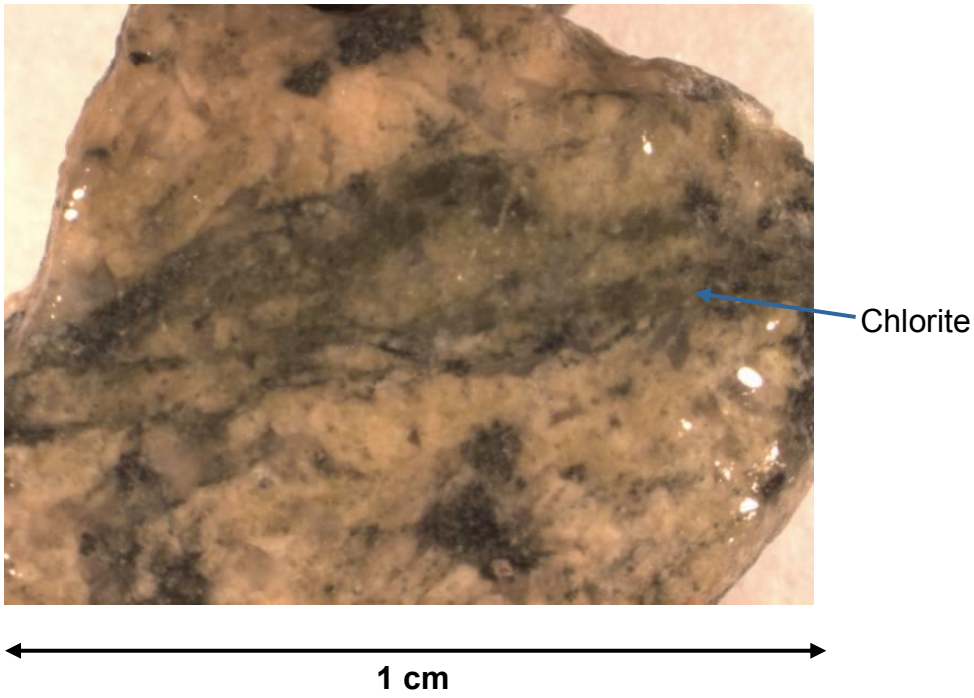

Figure 16 Photo of a pebble showing green alteration, probably chlorite, from the sample at a depth of 36.5-36.7m in core VTH2014-09.

5.3 Petrophysics – Magnetic Susceptibility

The magnetic susceptibility was measured across several different places on each of the core samples (**Figure 17**). Measurements were taken across the whole sample, and also across some of the larger pebbles in them.

Figure 17 Taking magnetic susceptibility measurements across one of the samples.

A graph of magnetic susceptibility vs. cumulative proportion of the samples shows the results of the petrophysical analysis (**Figure 18**). Data from the samples belonging to this dataset is shown in green and red. The points in green are the magnetic susceptibilities measured across the entire width of the core samples. The ones in red are the susceptibilities measured across some of the larger pebbles in the samples. The black points belong to a large dataset collected by the G.S.C. of magnetic susceptibilities of samples of the local bedrock, the Guichon Creek Batholith. The curves for the samples from this dataset and the samples from the bedrock in the study area are different. For the green and red curves belonging to this dataset, there are a lot of samples whose magnetic susceptibilities were on the order of 10^{-3}. This is seen on the graph by the large change across the proportion axis (MagSusc) at a magnetic susceptibility of about $1x10^{-3}$. However, for the samples from the bedrock, there are much fewer samples that had a magnetic susceptibility on

the order of 10^{-3}. There is not much of an increase in cumulative proportion of samples when the magnetic susceptibility is about $1x10^{-3}$. There are contrasting signatures for diamicton samples in the study area and bedrock samples in that area.

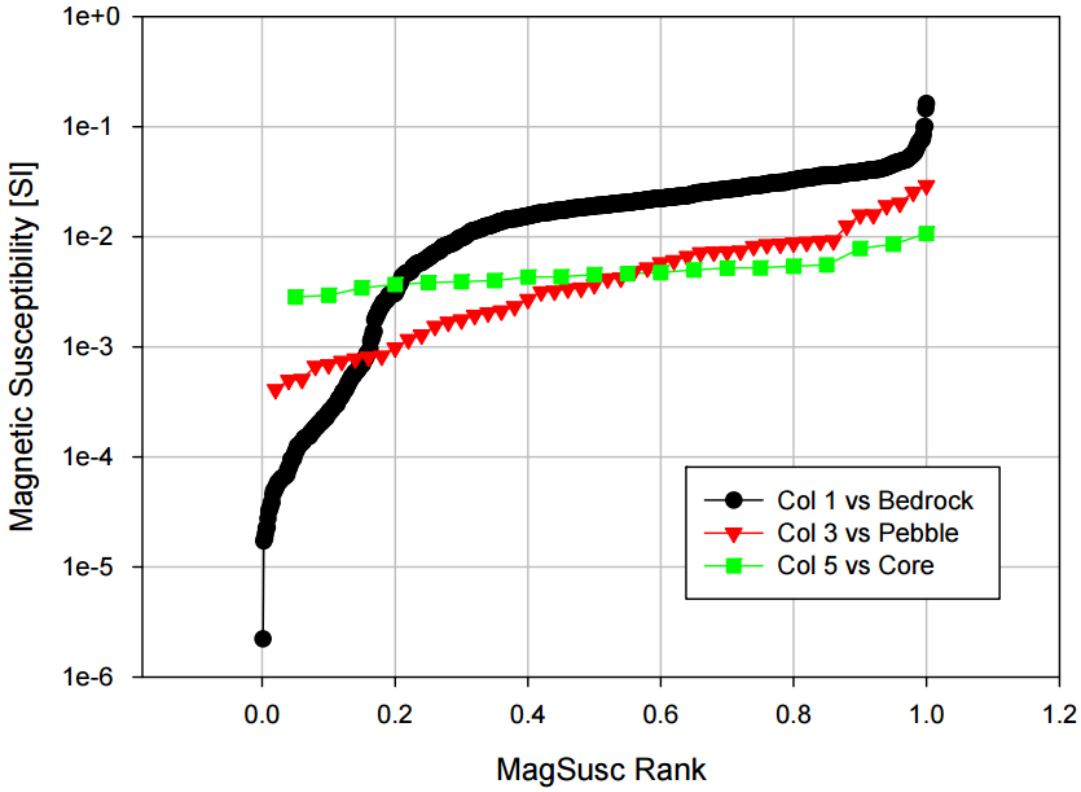

Figure 18 Plot of magnetic susceptibility vs. cumulative proportion of samples (MagSusc Rank).

The diamicton is therefore possibly not locally sourced, as long as the bedrock samples were representative. If the pebbles and matrix material had come from the same area it was deposited, then the distribution of magnetic susceptibility values would match, showing that the material is the same and the sediments are derived from the local bedrock. The sediments making up the diamicton therefore could possibly

have come from outside the Guichon Creek Batholith. The batholith is tens of kilometers across, so the sediments making up the diamicton might have come from a considerable distance away. Further investigation is needed to support the validity of this data.

6.0 Conclusions

This thesis has resulted in a preliminary stratigraphic framework of the unconsolidated sediments in the study area at Highland Valley. The Cenozoic sediment successions appear to be the result of several depositional environments. In the early phase of valley filling, there is evidence that the valley was occupied by a lake who received variable input of siliciclastic sediments and organic matter. Some of the coarsest layers could have been deposited in alluvial fan-deltas or braided rivers. Higher up the succession, there is clear evidence of proximity to a glacier for some of the stratified facies, along with a number of subglacial units. The main diamicton units are indeed confidently interpreted as subglacial traction tills due to the shape and composition of their clasts as well as their apparent over consolidation.

Sedimentological analysis of the upper till units of one of the cores shows that they are characterized by high density values and poor sorting. The density values can provide an upper limit to constrain geophysical inversion because the till unit is much more consolidated and stiff than all the other units observed in the cores. The lithology of the pebbles was characterized in order to be able to determine the provenance of the till. These pebbles are dominated by coarse-grained igneous rocks, indicating the main bedrock source is igneous. Evidence of alteration, including alteration commonly found in copper porphyry deposits, was found in the upper till units. This would suggest a local origin (Guichon Batholith).

However, the magnetic susceptibility measurements of the samples from the upper diamicton units show an order of magnitude difference with those of the till units and the local bedrock in the study area. Therefore, it indicates that although the pebble lithologies are mostly coarse-grained igneous with hydrothermal alteration assemblages consistent with porphyry style systems, the magnetic susceptibility results are different than those obtained so far on local bedrock. More research is needed to determine the cause of this discrepancy of magnetic susceptibility results and to establish with confidence the bedrock sources for the diamictons. The polymict nature (multiple lithologies) of the diamictons along with the lack of very angular clasts in these units and the typical shape of some of the clasts (e.g. bullet shape with truncated facet) support the interpretation that they have been transported by ice for some distance. Their matrix-supported texture indicates little reworking at the time of deposition and preferentially oriented clasts are likely caused by rotation of grains in the main direction of shear in a subglacial environment.

This work has provided the data to begin interpreting the distribution and physical properties of the stratigraphic units of the unconsolidated sediment successions at Highland Valley. It will help advance understanding of the Cenozoic depositional history in the area and its potential impact on the surficial footprint of deeply buried mineralized zones around HVC. It will be integrated in a "Common Earth Model" that is under development as part of a large research project (http://cmic-footprints.ca/). The data and interpretations from this thesis could improve exploration methods for finding new Cu-Mo deposits underneath both thick and thin sediment cover at Highland Valley as well as at other similar settings.

7.0 Future Work

This project will expand into a master's thesis. Further work will be done to expand and deepen the stratigraphic, sedimentological and petrophysical analysis of the unconsolidated sediments at Highland Valley. Many more cores from the study area will be logged in order to complete the stratigraphic framework. The remaining sedimentological units will be sampled and characterized in terms of physical properties, grain size, and lithology. Further petrophysical analysis will be done on them. Methods other than density and magnetic susceptibility may possibly be used.

Further work needs to be done to achieve a higher level of confidence on the mineral identities making up the pebbles. Mineral identities in this thesis were assigned based on most commonly occurring mineral that matches the physical properties observed. These mineral identities need to be verified. Thin sections of the pebbles and hyperspectral analysis would be useful to help do this.

Thin sections would also be a good way to see textures in the pebbles. This would help advance understanding of the geological history of the rock composing the pebbles and therefore aid in identifying provenance. Certain textures may also help determine whether certain minerals were originally present at the time of formation of the bedrock or whether they formed later and are the products of alteration.

References

- d'Angelo, Mike. (2016). *Geochemistry, petrography and mineral chemistry of the Guichon Creek and Nicola batholiths, southcentral British Columbia* [MSc]. Lakehead University.
- Ash, C. H., Reynolds, P. H., Creaser, R. A., and Mihalynuk, M. G. (2007). *40Ar-39Ar and Re-O Isotopic Ages for Hydrothermal Alteration and Related Mineralization at the Highland Valley Cu-Mo Deposit, Southwestern B.C.* British Columbia Geological Survey.
- Benn, D.I., and Evans, D.J.A. (2010). *Glaciers and Glaciation.* Second Edition. London: Hodder Education.
- Bergey, W.R. (2009). *Geological Report on the Highland Valley Property.* BC Geological Survey Assessment Report 31016.
- Bobrowsky, P. T., Kerr, D. E., Sibbick, S. J., and Newman, K. (1993). *Drift Exploration Studies, Valley Copper Pit, Highland Valley Copper Mine, British Columbia: Stratigraphy and Sedimentology.* British Columbia Geological Survey.
- Boggs, S. (2006). *Principles of Sedimentology and Stratigraphy.* Fourth Edition. Upper Saddle River, New Jersey: Pearson Education, Inc. p. 51-64.
- Bouzari, F., Hart, C. J. R., Barker, S., and Bissig, T. (2011). *Porphyry Indicator Minerals (PIMS): A New Exploration Tool for Concealed Deposits in South-Central British Columbia.* Geoscience BC Report 2011.
- Casselman, M.J., McMillan, W.J., Newman, K.M., (1995). *Highland Valley porphyry copper deposits near Kamloops, British Columbia: A review and update with emphasis on the Valley deposit: Porphyry Deposits of the Northwestern Cordillera of North America.* The Canadian Institute of Mining and Metallurgy, Paper 8, p.161-191.

- Enkin, R. (2016). Paleomagnetism and Petrophysics Laboratory and Section Head, Sedimentary Systems and Processes, Geological Survey of Canada Pacific, Natural Resources Canada, Government of Canada.
- Evans, D.J.A., and Benn, D. I. (2004). *A Practical Guide to the Study of Glacial Sediments.* London, U.K.: Hodder Education. P. 42.
- Fulton, R.J. (1975). *Quaternary geology and geomorphology, Nicola-Vernon area, British Columbia (82 L W 1/2 and 92 I E 1/2).* Geological Survey of Canada, Memoir 380.
- Fulton, R.J. (1969). *Glacial lake history, southern Interior Plateau, British Columbia.* Geological Survey of Canada, Paper 69-37.
- Fulton, R.J. (1967). *Deglaciation studies in Kamloops region, an area of moderate relief, British Columbia.* Geological Survey of Canada, Bulletin 154.
- McMillan, W.J., Anderson, R. G., Chan, R., and Chow, W. (2009*). Geology and mineral occurrences (MINFILE), the Guichon Creek Batholith and Highland Valley porphyry copper district, British Columbia.* Geological Survey of Canada, Open File 6079, 2 sheets, doi:10.4095/248060.
- McMillan, W.J. (1985). *Geology and ore deposits of the Highland Valley Camp.* Field guide and reference manual series / Geological Association of Canada, Mineral Deposits Division; no. 1. Geological Association of Canada. One folded map in pocket.
- Plouffe, A., and Ferbey, T. (2015).
    - [A] *Surficial geology, Gnawed Mountain area, British Columbia (Parts of NTS 092I/6,7,10,11).* Geoscience Map.
    - [B] *Till composition near Cu-porphyry deposits in British Columbia: Highlights for mineral exploration; in TGI 4 – Intrusion Related Mineralisation Project: New Vectors to Buried Porphyry-Style Mineralisation*. (ed.) N. Rogers; Geological Survey of Canada, Open File 7843, p. 15-37.

- Plouffe, A., Ferbey, T., Levson, V. M., and Bond, J. D. (2012). *Glacial history and drift prospecting in the Canadian Cordillera: recent developments.* Geological Survey of Canada, Open File 7261, 51 pages, doi:10.4095/292101.
- Preto, V. A. (1979). *Geology of the Nicola Group between Merritt and Princeton.* British Columbia Ministry of Energy, Mines and Petroleum Resources, Bulletin 69.
- Sillitoe, R. H. (2010). *Porphyry Copper Systems.* Society of Economic Geologists, Inc. Economic Geology v.105, p. 3-41.
- Taylor, R., (2009). *Ore Textures: Recognition and Interpretation.* Springer Science & Business Media.
- *Integrated Multi-Parameter Footprints of Ore Systems: The Next Generation of Ore Models.* (c2016). [accessed April 3, 2016]. https://cmic-footprints.ca/.

Appendix

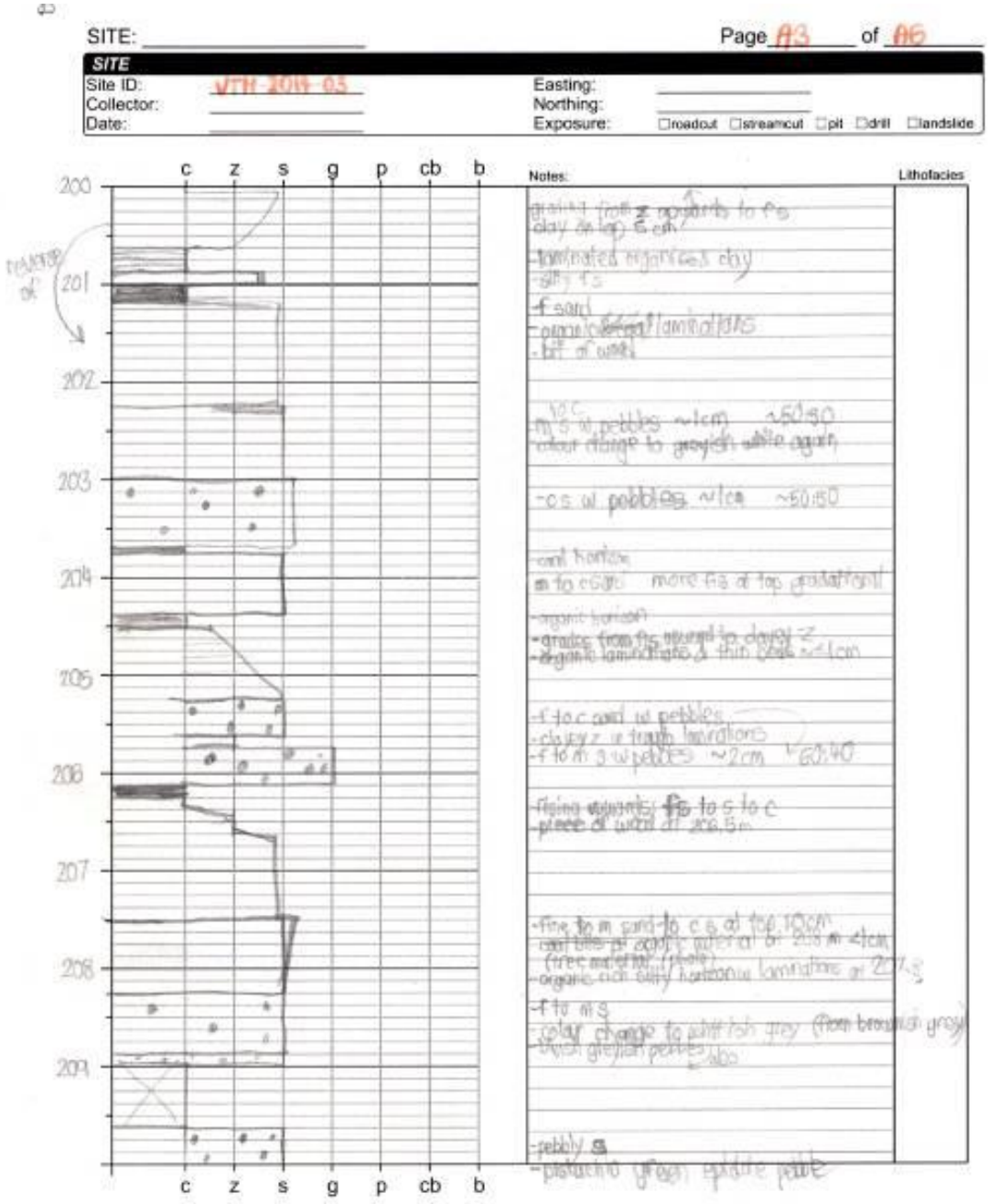

Figure 1 An example of the logging method of lithofacies analysis done on each core.

Figure 2a Photo of the thick Fl (finely laminated silts and clays) lithofacies unit of core VTH2014-03, at a depth of 96.9-104.0m. Lithofacies code from Evans and Benn (2004).

Figure 2b Close up photo of an Fl (finely laminated silts and clays) lithofacies unit of core VTH2014-03, at a depth of about 34m. Lithofacies code from Evans and Benn (2004).

Figure 3 Photo of a Sm (massive sand) lithofacies unit of core VTH2014-03, at a depth of 35.6-58.1m. Lithofacies code from Evans and Benn (2004).

Figure 4 Photo of the transition from Sm (massive sand) lithofacies unit to Dmm (matrix-supported, massive diamicton) and Bcm (clast-supported, massive boulders) units of core VTH2014-03, at a depth of 0-18.7m. Lithofacies code from Evans and Benn (2004).

Figure 5a Photo of the alternating Sm (massive sand) and Fm (massive silts and clays) lithofacies units of core VTH2014-06, at a depth of 179.0-192.5m. Lithofacies code from Evans and Benn (2004).

Figure 5b Photo of an Sl (sand with horizontal and draped laminations) lithofacies unit and rounded pebble of core VTH2014-06, at a depth of 73.3m. Lithofacies code from Evans and Benn (2004).

Figure 6 Photo of an Sl (sand with horizontal and draped laminations) lithofacies unit and coal lenses of core VTH2014-06, at a depth of 72.5-165.5m. Lithofacies code from Evans and Benn (2004).

Figure 7 Photo of Sm (massive sand) and Bcm (clast supported, massive boulders) lithofacies units of core VTH2014-06, at a depth of 29.1-46.5m. Lithofacies code from Evans and Benn (2004).

Figure 8 Photo of coal lenses in Flv (finely laminated silts and clays with rhythmites) lithofacies unit of core VTH2014-09, at a depth of 212.0-225.5m. Lithofacies code from Evans and Benn (2004).

Figure 9 Photo of the lower Dmm (matrix-supported, massive diamicton) lithofacies unit of core VTH2014-09, at a depth of 141.5-152.0m. Lithofacies code from Evans and Benn (2004).

Figure 10 Photo of the upper Sm (massive sand) lithofacies unit of core VTH2014-09, at a depth of 107.7-133.5m. GRmc (massive granules with isolated, outsize clasts) are visible. Lithofacies codes from Evans and Benn (2004).

Figure 11a Photo of one of the upper Dmm (matrix-supported, massive diamicton) lithofacies units of core VTH2014-09, at a depth of 33.9-40.9m. Lithofacies code from Evans and Benn (2004).

Figure 11b A close-up image of one of the Dmm (matrix-supported, massive diamicton) units from drillcore VTH 2014-09. Note the angularity of the framework clasts, the silty texture of the matrix and the stiffness.

Figure 12 Photo of a bullet-shaped, rounded clast from the upper Dmm (matrix-supported, massive diamicton) lithofacies unit of core VTH2014-09 shown in figure 19. Lithofacies code from Evans and Benn (2004).

Figure 13 Photo of preferentially oriented clasts in one of the upper Dmm (matrix-supported, massive diamicton) lithofacies units of core VTH2014-09, at a depth of 51.9-52.3m. Lithofacies code from Evans and Benn (2004).

Figure 14 Photo of the uppermost Bcm (clast-supported, massive boulders) and Gm (clast-supported, massive gravel) lithofacies unit of core VTH2014-09, at a depth of 0-33.5m. Lithofacies code from Evans and Benn (2004).

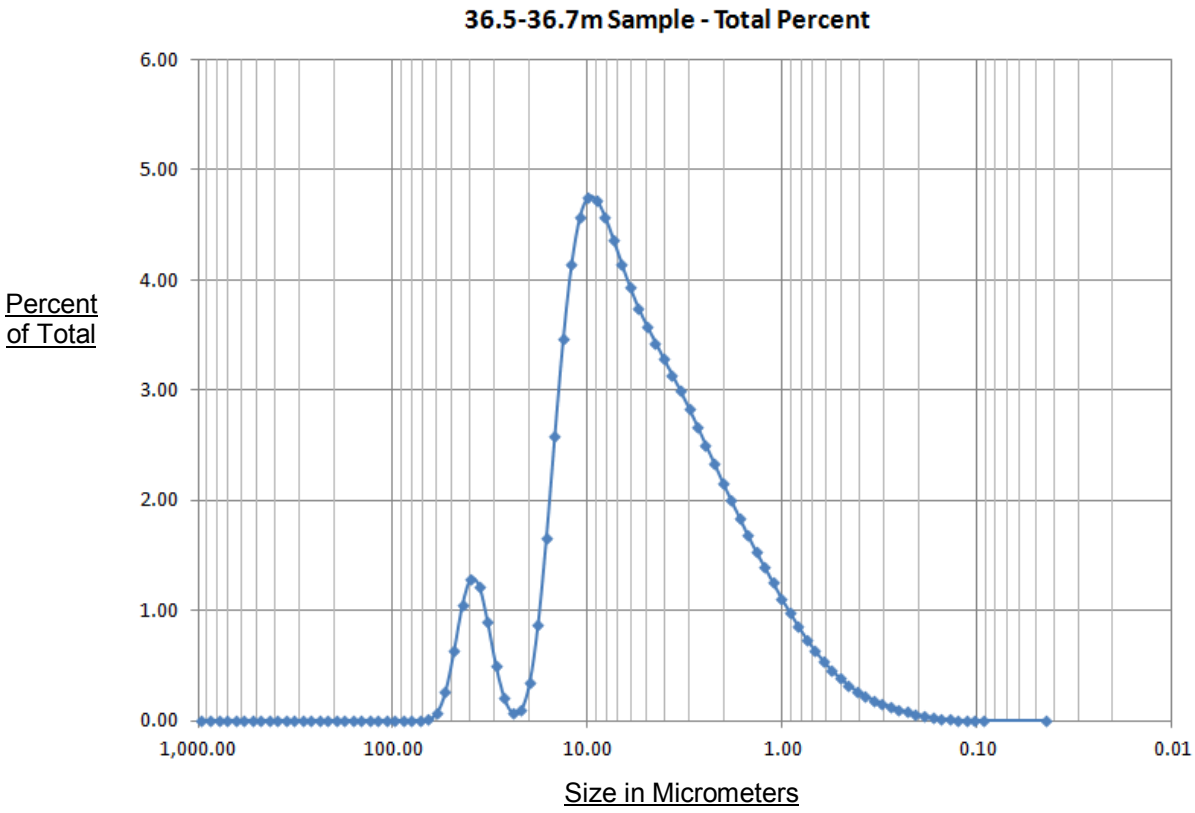
36.5-36.7m Sample - Total Percent
Percent of Total
6.00
5.00
4.00
3.00
2.00
1.00
0.00
1,000.00
100.00
10.00
1.00
0.10
0.01
Size in Micrometers

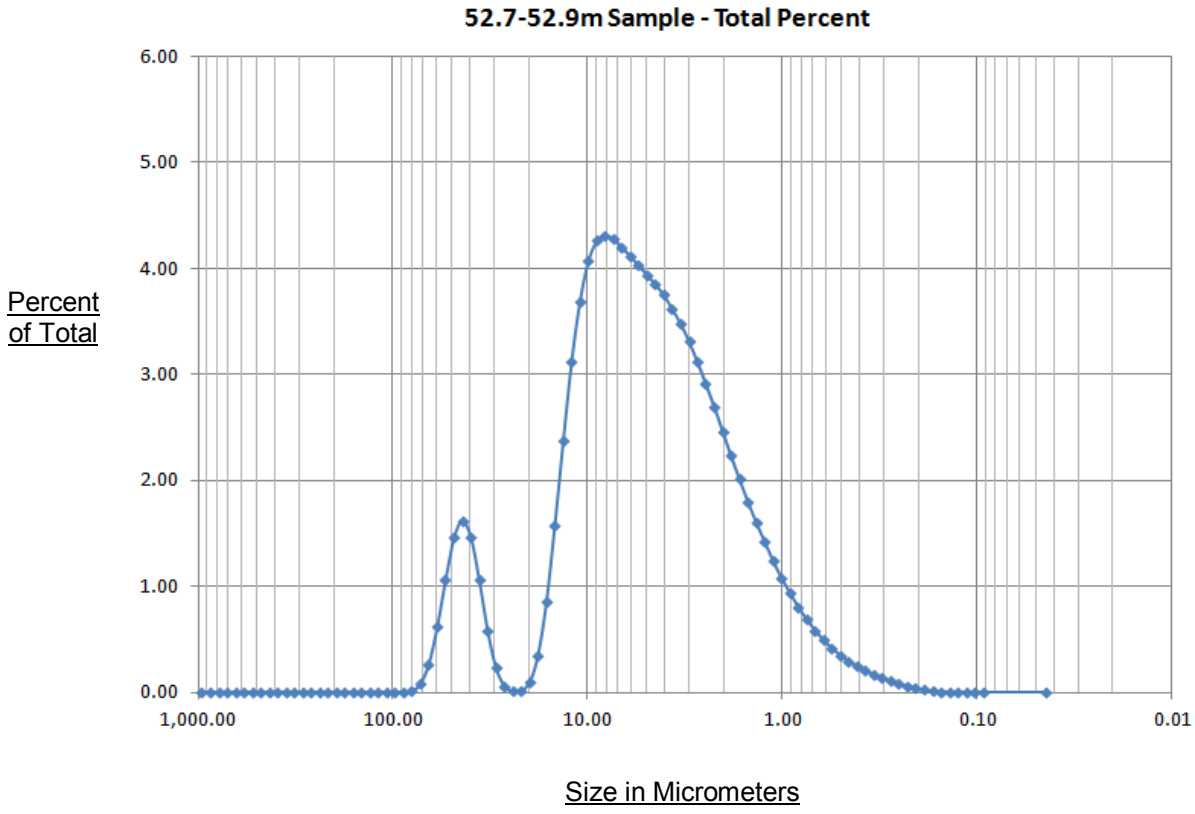
52.7-52.9m Sample - Total Percent
Percent of Total
6.00
5.00
4.00
3.00
2.00
1.00
0.00
1,000.00
100.00
10.00
1.00
0.10
0.01
Size in Micrometers

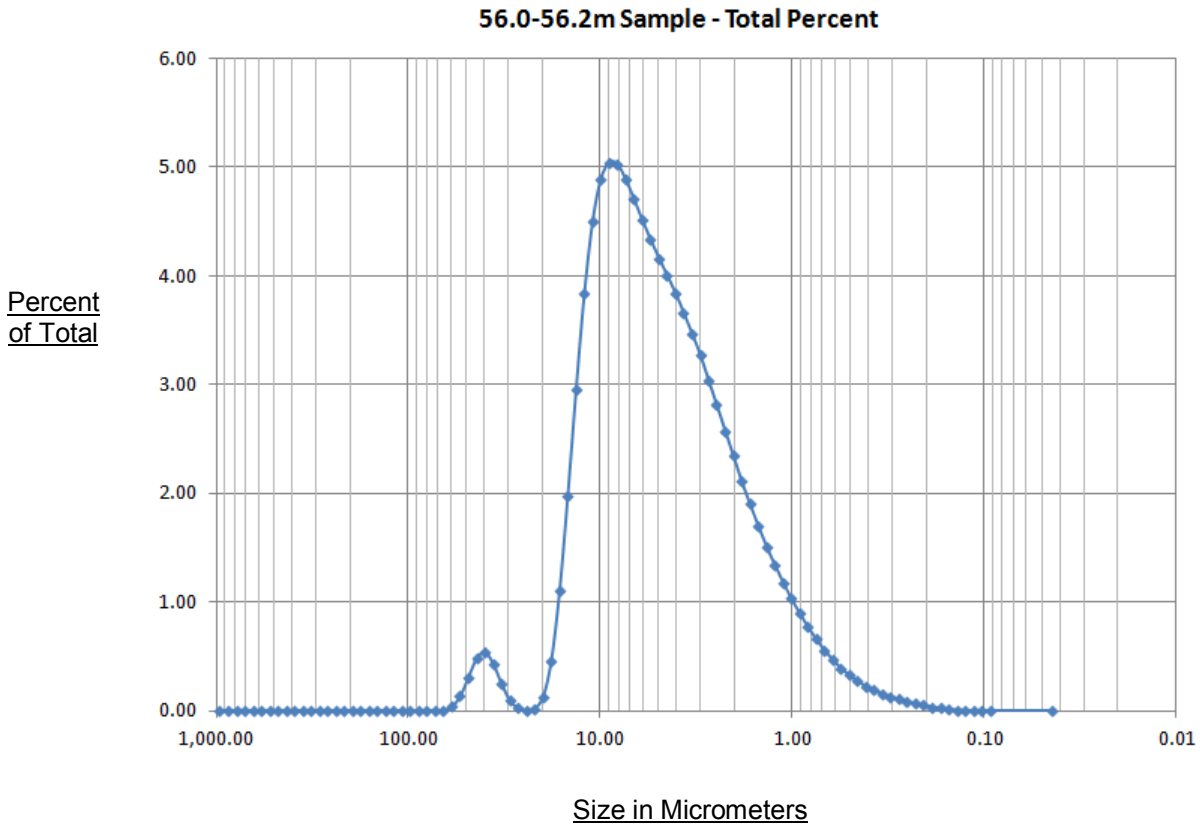
56.0-56.2m Sample - Total Percent
Percent of Total
6.00
5.00
4.00
3.00
2.00
1.00
0.00
1,000.00
100.00
10.00
1.00
0.10
0.01
Size in Micrometers

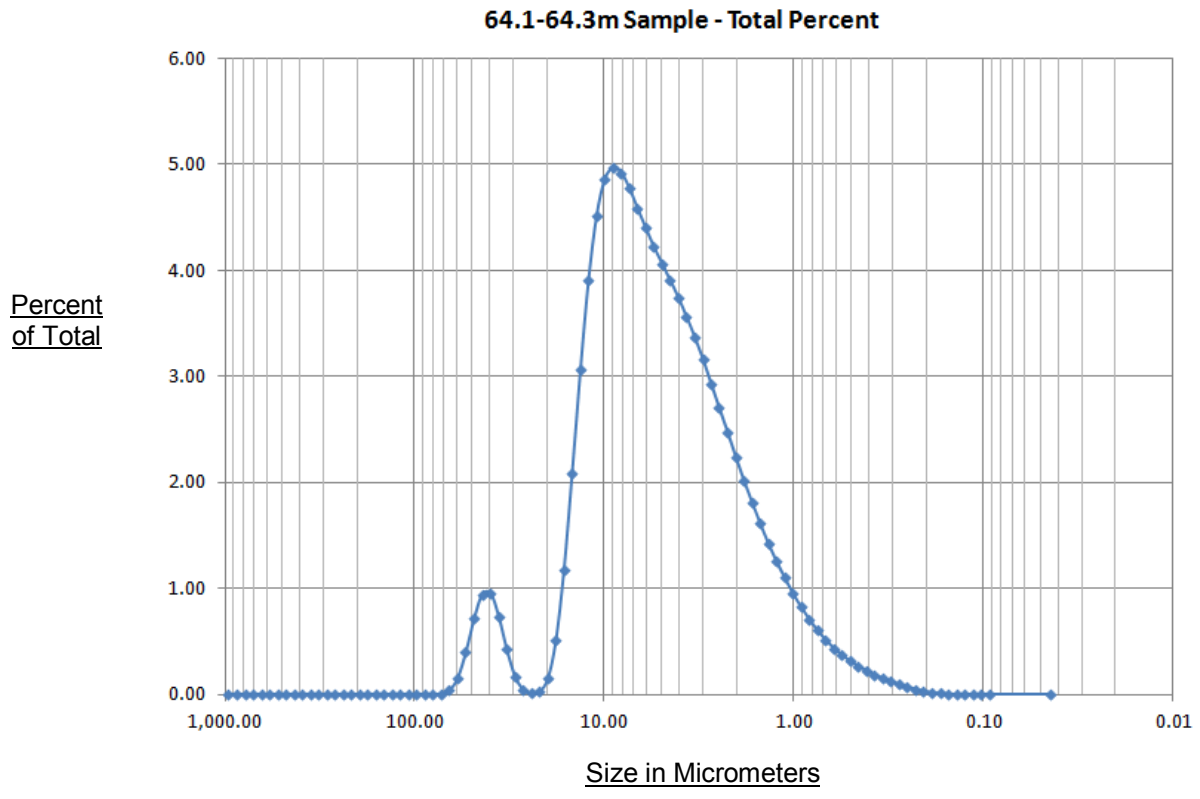
64.1-64.3m Sample - Total Percent
Percent of Total
6.00
5.00
4.00
3.00
2.00
1.00
0.00
1,000.00
100.00
10.00
1.00
0.10
0.01
Size in Micrometers

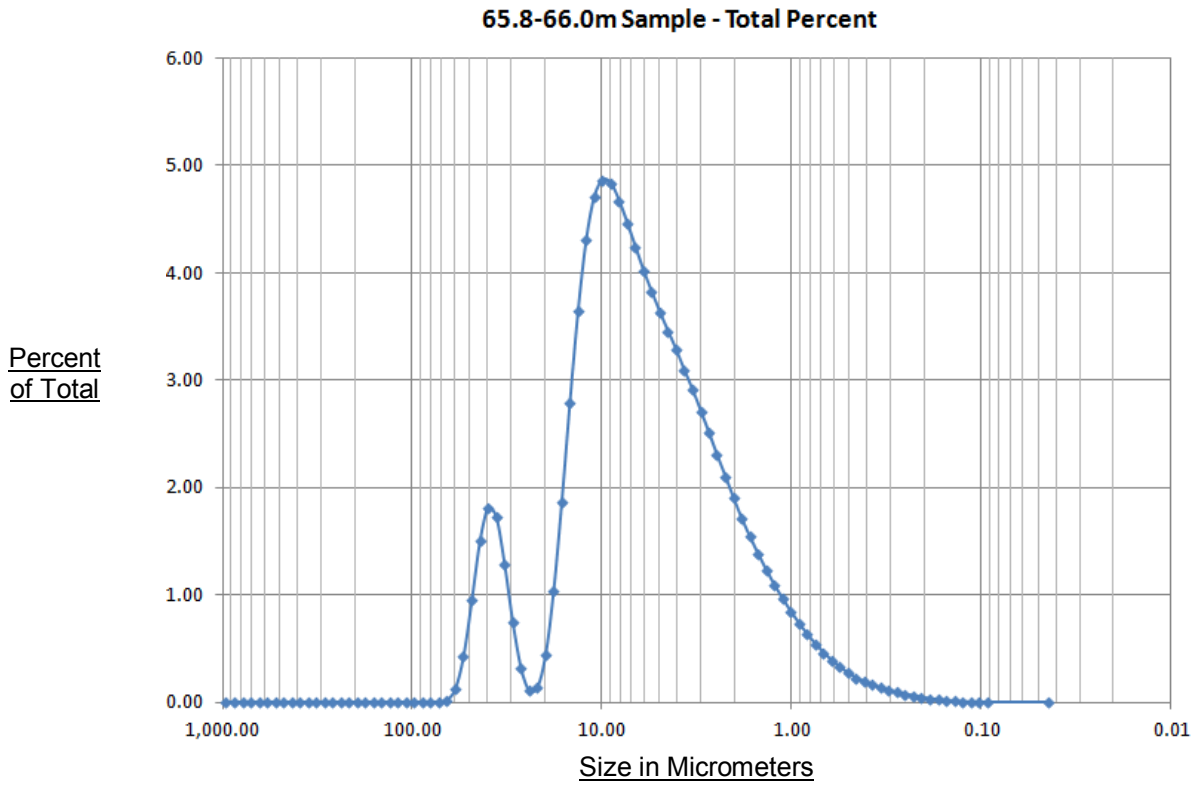

Figure 15 Graph of percent of total vs. size of grain for the <63µm fraction of the samples.

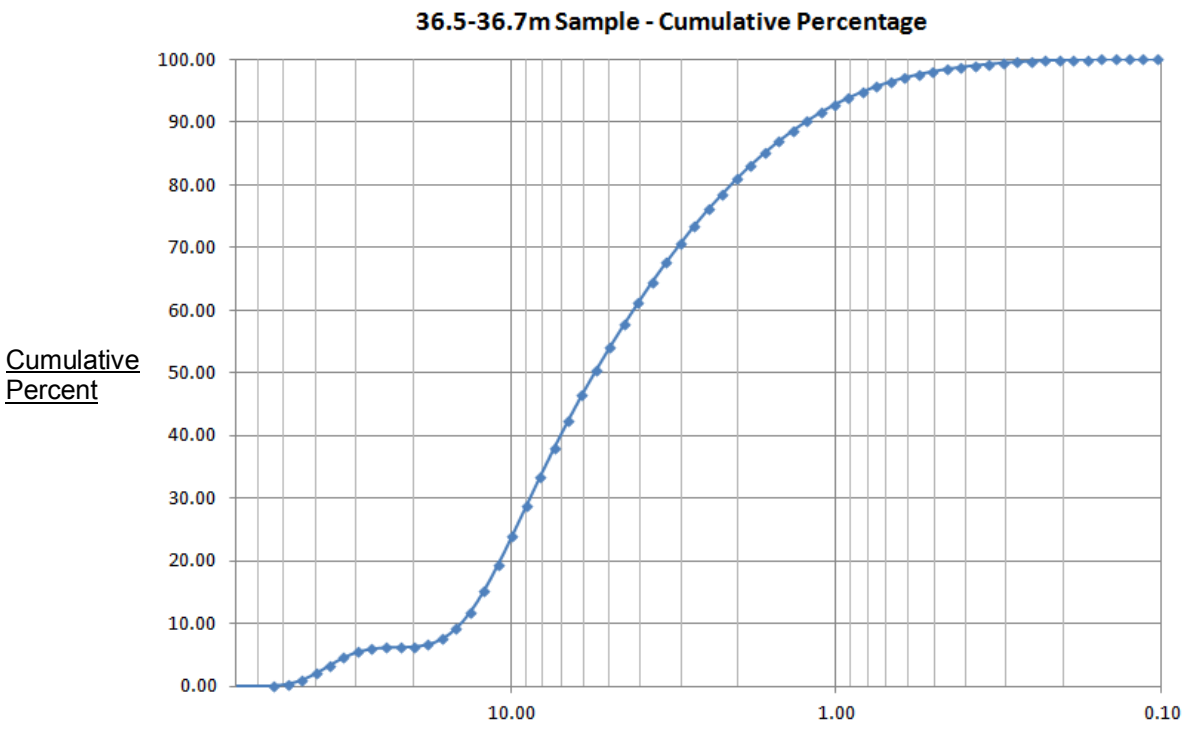
36.5-36.7m Sample - Cumulative Percentage
100.00
90.00
80.00
70.00
60.00
50.00
40.00
30.00
20.00
10.00
0.00
10.00
1.00
0.10
Cumulative Percent
Size in Micrometers

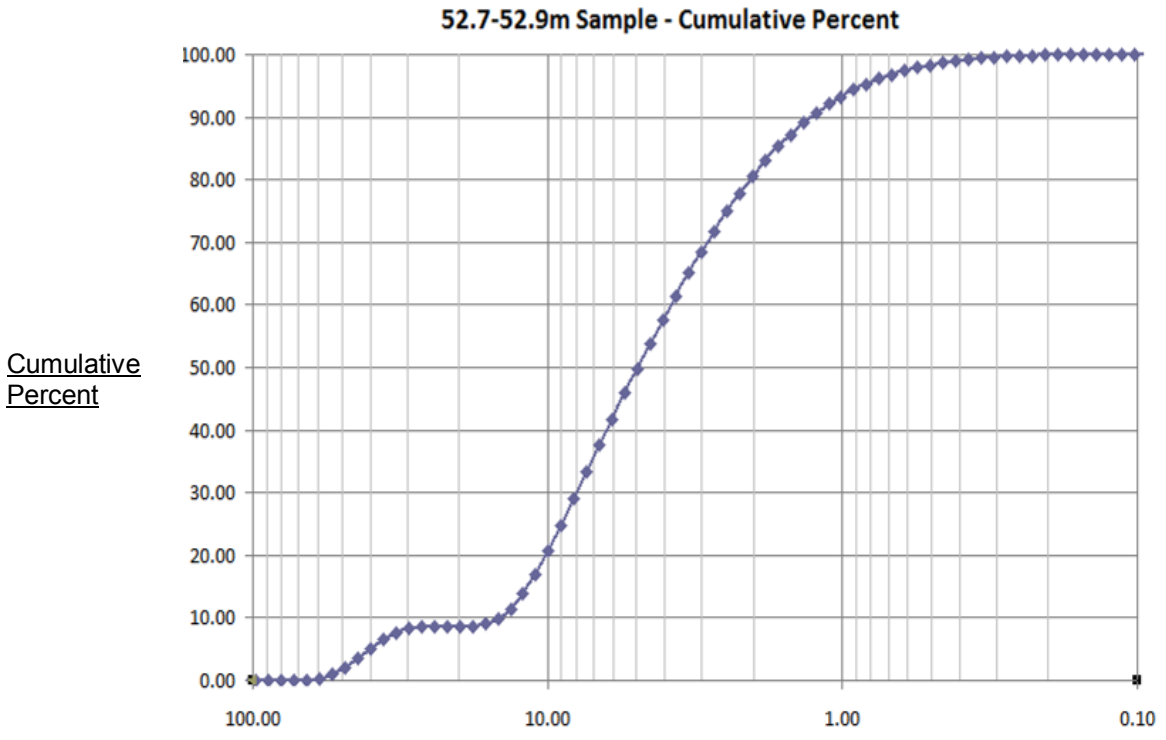
52.7-52.9m Sample - Cumulative Percent
100.00
90.00
80.00
70.00
60.00
50.00
40.00
30.00
20.00
10.00
0.00
100.00
10.00
1.00
0.10
Cumulative Percent
Size in Micrometers

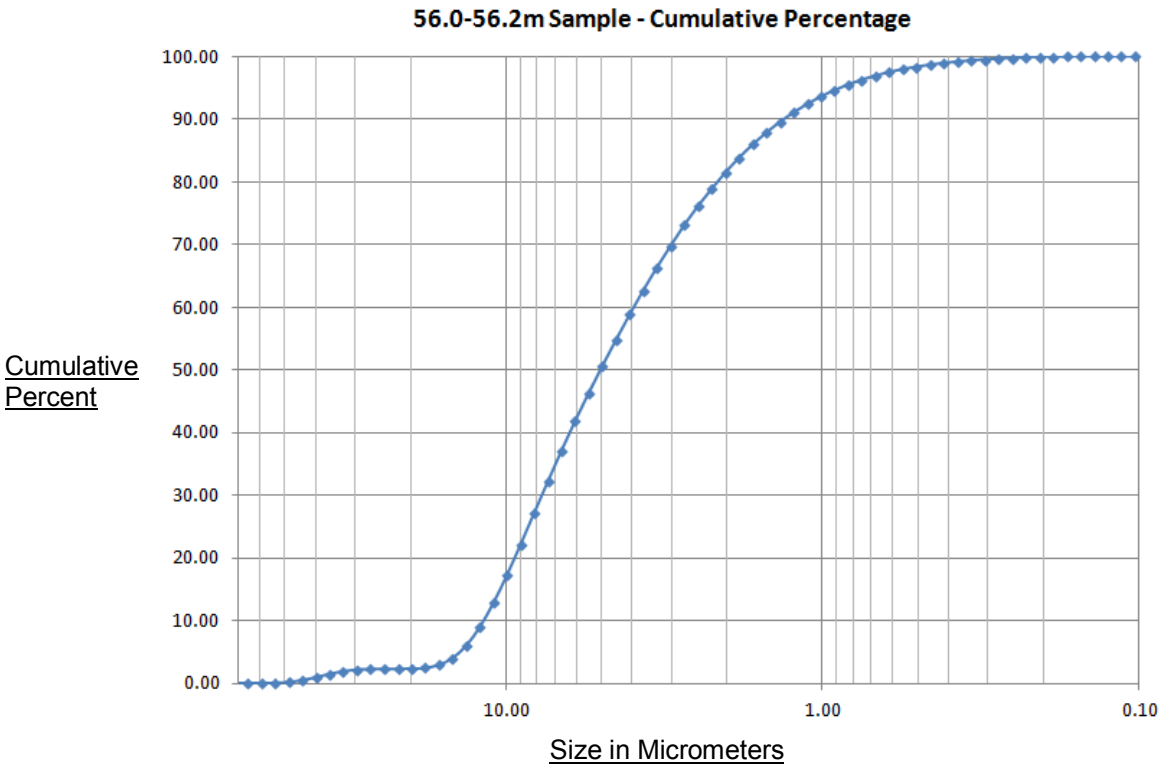
56.0-56.2m Sample - Cumulative Percentage
100.00
90.00
80.00
70.00
60.00
50.00
40.00
30.00
20.00
10.00
0.00
10.00
1.00
0.10
Cumulative Percent
Size in Micrometers

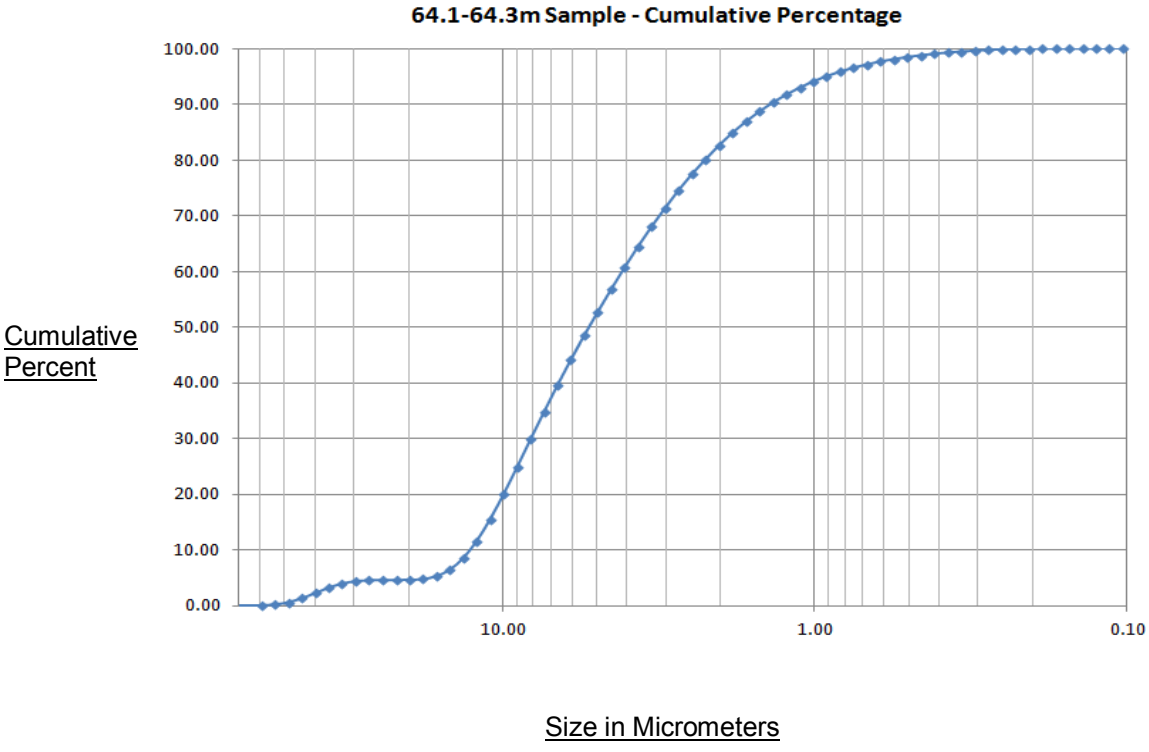
64.1-64.3m Sample - Cumulative Percentage
100.00
90.00
80.00
70.00
60.00
50.00
40.00
30.00
20.00
10.00
0.00
10.00
1.00
0.10
Cumulative Percent
Size in Micrometers

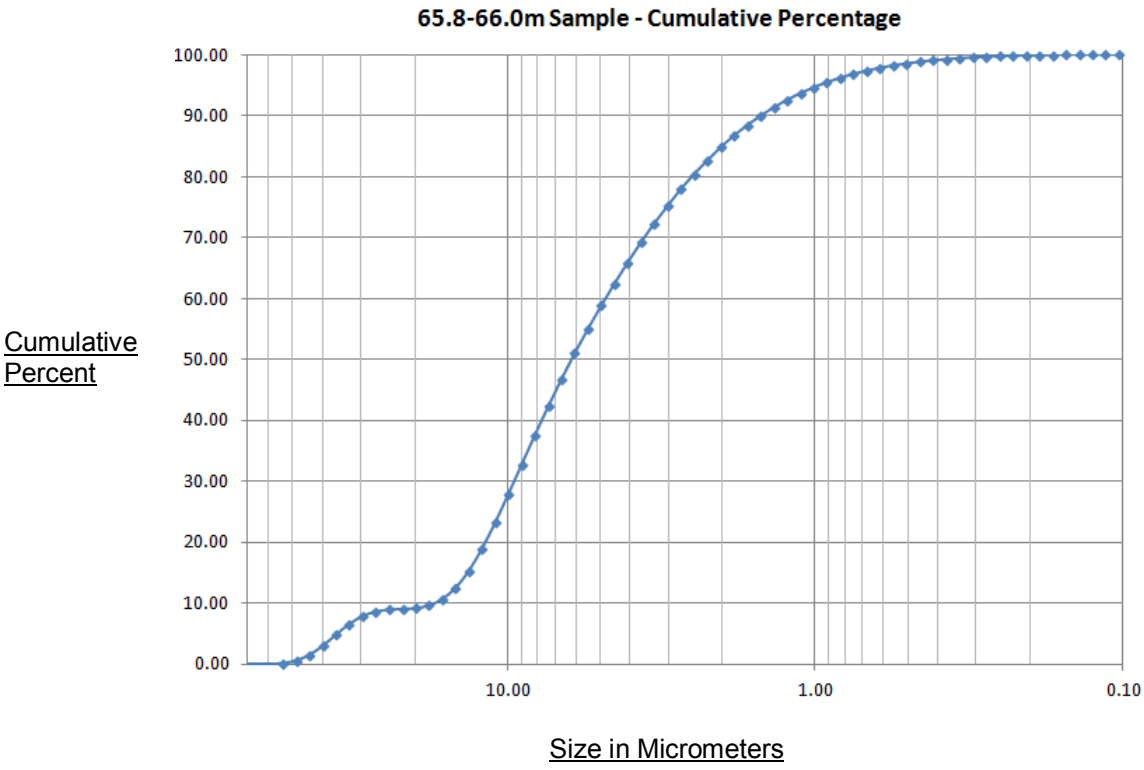

Figure 16 Graph of cumulative percent vs. size of grain for the <63µm fraction of the samples.